

1169-28158  
NASA Col-100470



NATIONAL AERONAUTICS AND SPACE ADMINISTRATION

EARTH RESOURCES SURVEY PROGRAM

TECHNICAL LETTER NASA-96

VACUUM ULTRAVIOLET MEASUREMENTS OF REFLECTANCE  
AND LUMINESCENCE FROM VARIOUS ROCK SAMPLES

By

H. V. Watts

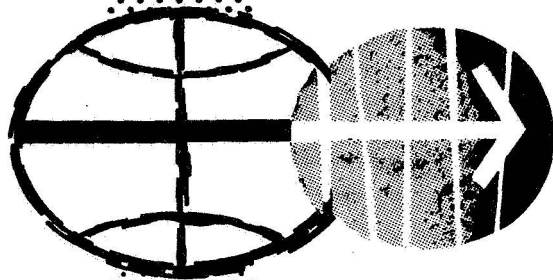
and

H. J. Goldman

IIT Research Institute  
Chicago, Illinois

January 1968

Prepared by the Geological Survey for the  
National Aeronautics and Space Administration (NASA)  
under NASA Work Order No. T-65757



MANNED SPACECRAFT CENTER  
HOUSTON, TEXAS

NR-05-00-000-0096



UNITED STATES  
DEPARTMENT OF THE INTERIOR  
GEOLOGICAL SURVEY  
WASHINGTON, D.C. 20242

Interagency Report  
NASA-96  
January 1968

Mr. Robert Porter  
Acting Program Chief,  
Earth Resources Survey  
Code SAR - NASA Headquarters  
Washington, D.C. 20546

Dear Mr. Porter:

Transmitted herewith is one copy of:

INTERAGENCY REPORT NASA-96  
VACUUM ULTRAVIOLET MEASUREMENTS OF  
REFLECTANCE AND LUMINESCENCE FROM  
VARIOUS ROCK SAMPLES\*

by

H. V. Watts\*\*

and

H. J. Goldman\*\*

The U.S. Geological Survey has released this report in open files. Copies are available for consultation in the Geological Survey Libraries, 1033 GSA Building, Washington, D.C. 20242; Building 25, Federal Center, Denver, Colorado 80225; 345 Middlefield Road, Menlo Park, California 94025; and 601 East Cedar Avenue, Flagstaff, Arizona 86001.

Sincerely yours,

William A. Fischer  
Research Coordinator  
Earth Orbiter Program

\*Work performed under Work Order No. T-65757

\*\*IIT Research Institute, Chicago, Illinois

UNITED STATES  
DEPARTMENT OF THE INTERIOR  
GEOLOGICAL SURVEY

INTERAGENCY REPORT NASA-96

VACUUM ULTRAVIOLET MEASUREMENTS OF  
REFLECTANCE AND LUMINESCENCE FROM  
VARIOUS ROCK SAMPLES\*

by

H. V. Watts\*\*

and

H. J. Goldman\*\*

January 1968

Prepared by the U.S. Geological Survey  
for the National Aeronautics and Space  
Administration (NASA)

\*Work performed under Work Order No. T-65757

\*\*IIT Research Institute, Chicago, Illinois

CONTENTS

	<u>Page</u>
I. INTRODUCTION	1
II. EXPERIMENTAL TECHNIQUE	3
A. Sample Surface Preparation	3
B. Instrumentation	5
C. Measurement Geometry	6
D. Measurement Methods and Standardization	9
III. DATA AND DISCUSSION	13
IV. OBSERVATIONS	21
V. CONCLUSIONS AND PLANS FOR FUTURE WORK	23
REFERENCES	24
APPENDIX: DATA CURVES	A-1

### LIST OF FIGURES

	<u>Page</u>
Figure 1: Geometry for Type I Measurements	7
Figure 2: Geometry for Type II Measurements	8
Figure 3: Copper Reference Data	11

### LIST OF TABLES

Table 1: Reflectance Samples	4
------------------------------	---

VACUUM ULTRAVIOLET MEASUREMENTS OF  
REFLECTANCE AND LUMINESCENCE FROM  
VARIOUS ROCK SAMPLES

I.        INTRODUCTION

This study is a continuation of the work reported in "Reflectance of Rocks and Minerals to Visible and Ultraviolet Radiation," Technical Letter, NASA-32, July, 1966, (Ref. 1), in which reflectance data were obtained from 2300A to 7000A with a Cary Model 14 MR recording spectrophotometer utilizing the Model 1411 diffuse reflectance attachment. The overall objective of these studies is to determine if there are significant differences in the spectral reflectance or emission from various geological materials which may be used for identification and/or differentiation purposes in remote sensing applications. The two factors which distinguish the current study are:

1. The samples were in an evacuated chamber during the measurements. This permitted the short wavelength range to be extended into the so-called "vacuum ultraviolet," i.e., wavelengths shorter than 2000A. In order to facilitate comparison with the previous study the spectral region from 2300A to 3000A was repeated.
2. Measurements were made with both monochromatic and broad band sample illumination utilizing a corresponding broad band and monochromatic detection.

This permitted the separation of the reflection and luminescence components, which was not possible in the previous study.

## II. EXPERIMENTAL Techniques

### A. Sample Surface Preparation

The eleven samples selected for study and their source localities are listed in Table 1. Each sample was cut to form a one inch by one inch slab of about one-quarter inch thickness. One surface of the slab was ground with 320 silicon carbide (30 micron particle size). This surface is designated as the "ground" surface. The other surface was further ground with W8 aluminum oxide (8 micron particle size) and then polished with Linde "B" (0.05 micron) on one-quarter inch thick felt. This surface is designated as the "polished" surface. After grinding or polishing, the surfaces were rinsed in absolute alcohol immediately prior to insertion in the sample measurement chamber. Care was taken so that the sample surfaces were not touched or contaminated in handling.

Except for the pumice sample the surfaces of the eight rocks were the same as those used in the previous study of Reference 1. The pumice could not be polished because of its porous vesicular nature. In the slab size required, the pumice samples were somewhat fragile and, in fact, two samples broke in the process of mounting in the sample holder.

The meteorite samples, especially the Coarse Octahedrite, were more difficult to size and work. In the previous study the meteorite was simply cut into two parts, and the cut surface of one part was ground and the opposite surface part of the cut was polished. The requirement of a small slab sample



Table 1

REFLECTANCE SAMPLES

Code No.	Type	Source Locality
Li 2617	Biotite Granite	Pike's Peak, Colorado
Li 3760	Rhyolite	Nathrop, Colorado
Li 3905	Monzonite	Tintie, Utah
Li 3770	Diorite	Timichi Creek, Gunnison, Colorado
Li 4238	Gabbro	Everton, New York
Li 2288	Basalt	Whatcomb Co., Washington
E 18086	Dunite	Buck Creek, Macon Co., No. Carolina
Li 1832	Obsidian	Regla Falls, Aidalgo, Mexico
Li 1221	Pumice	Latacunga, Ecuador
Me 1990	Hypersthene Chondrite (stony)	Colby, Clark Co., Wisconsin
Me 1252	Coarse Octahedrite (iron-nickel)	Canon Diablo, Coconino Co., Arizona

to fit into the vacuum sample chamber in this work required more cutting and in so doing the actual surfaces used were not the same as those previously examined. The Coarse Octahedrite (iron-nickel) appeared as a metallic surface which took a high polish; the Hypersthene Chondrite surface had a mottled appearance with some small, shiny metallic spots.

#### B. Instrumentation

A Jarrell Ash Model 78-650 one-half meter scanning vacuum grating monochromator of the Seya-Namioka type was used. The grating size is 38 x 38 mm with 30,000 lines per inch, blazed for use in the 500A to 3000A range. Monochromator slit widths of about 0.3 mm were used, which with the instrument dispersion of 17A per mm gave a band pass of about 5A.

The source was a Tanaka-Type capillary discharge tube (Jarrell Ash Model 45-202) exciting ultra pure (99.999%) hydrogen at 15,000 volts AC and 500 milliamps. A windowless configuration was used, i.e., the source gas was differentially pumped through the entrance slit of the monochromator. In normal operation the monochromator chamber pressure was  $10^{-3}$  mm Hg and the source chamber was filled with hydrogen at about 0.5 to 1 mm pressure.

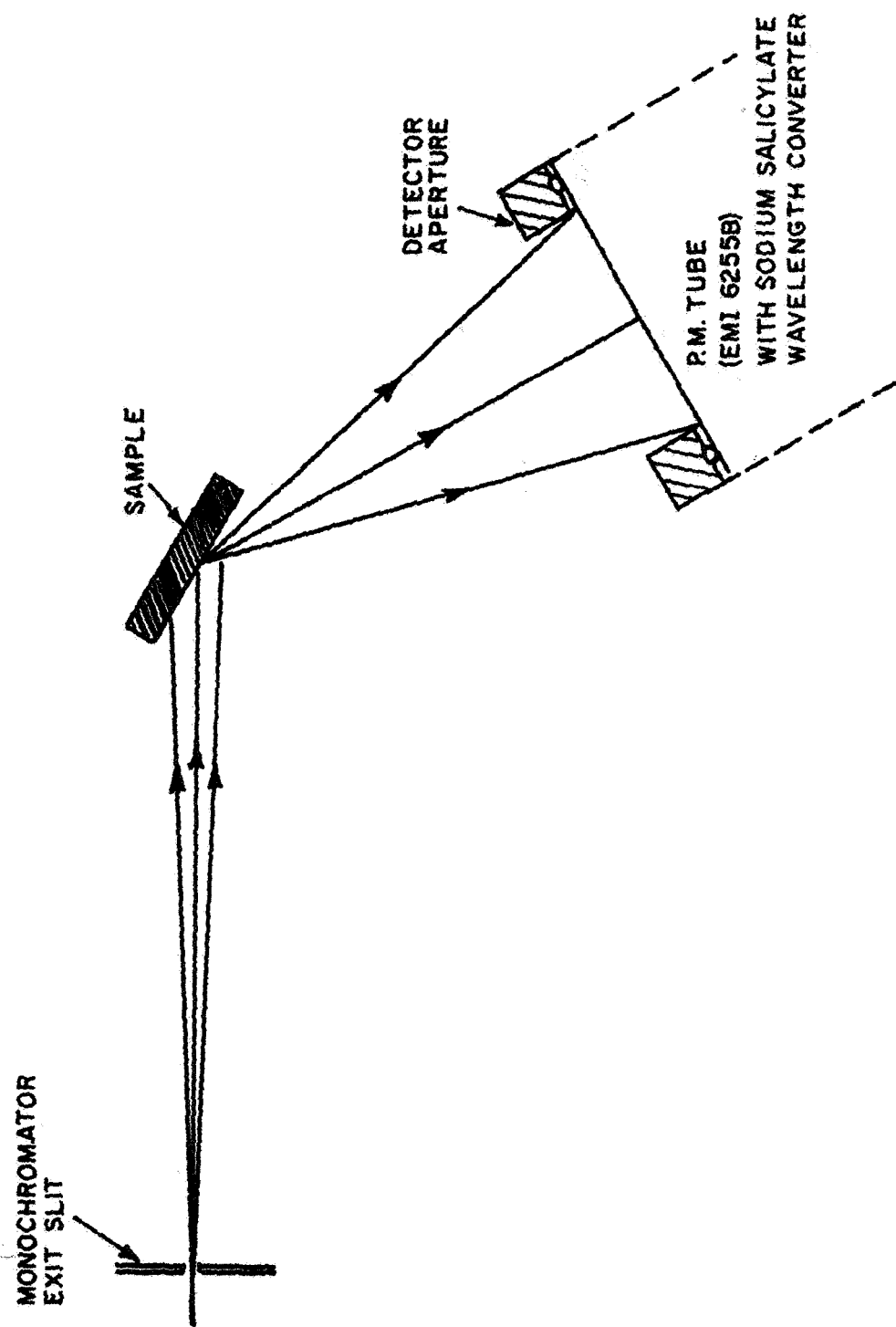
The detector was an EMI 6255B multiplier phototube with an S-13 response. A thin coating of sodium salicylate was used to extend the standard S-13 response in visible and near ultraviolet to wavelengths as short as 900Å in the vacuum ultraviolet.

The associated circuitry, high voltage supply, micro-micro ammeter and recorder, were the standard Jarrell Ash instrument package. The multiplier phototube had a dark current of the order of  $10^{-11}$  amps at 1000 volts. Most of the data measurements produced signals of at least  $10^{-9}$  amps so that the detectability was generally good.

### C. Measurement Geometry

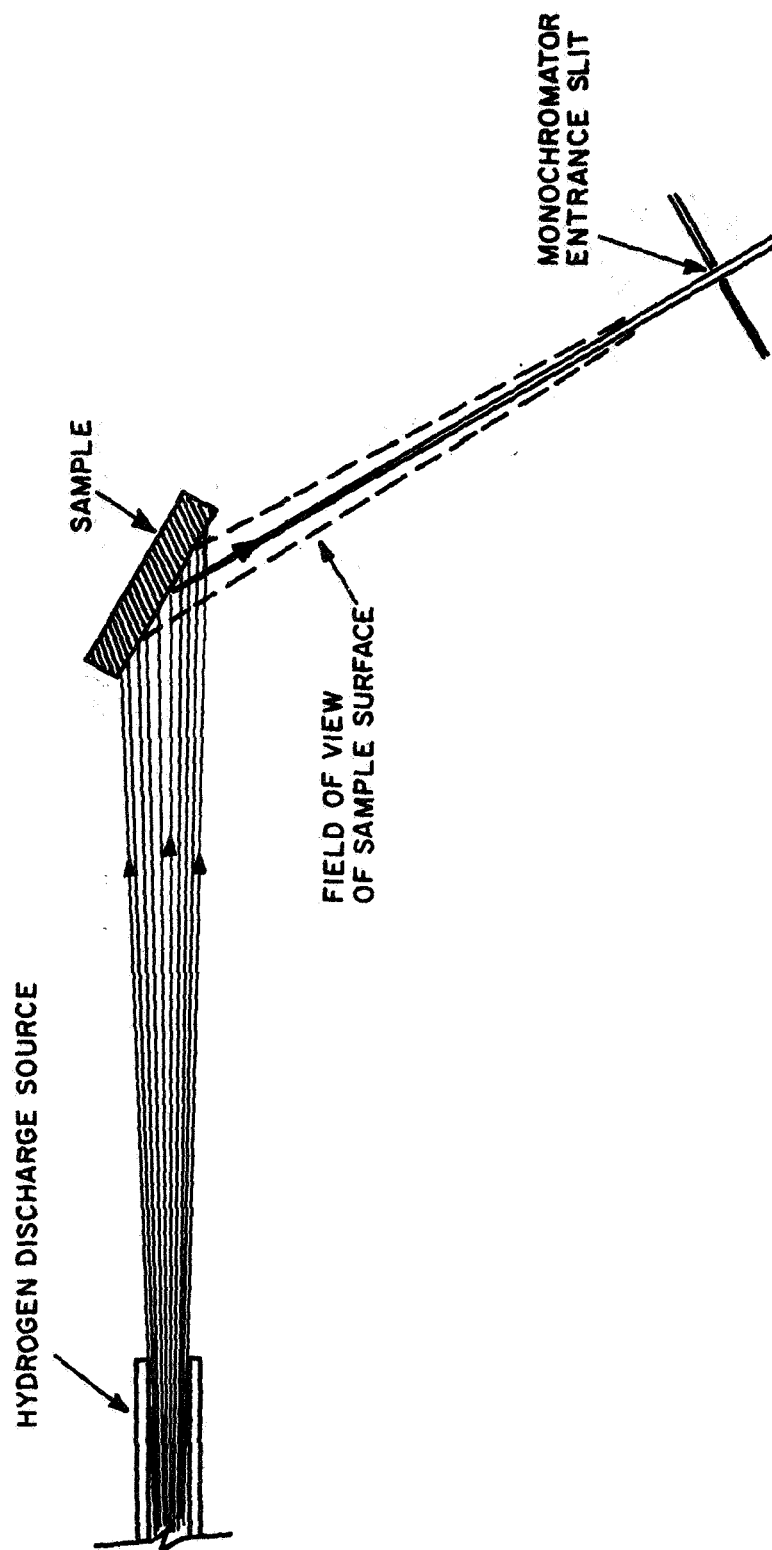
A vacuum tight sample chamber was constructed to hold six samples on a rotatable hexagonal wheel. This chamber could be attached to either the entrance or exit slit of the monochromator; either the source or the detector could be attached to the other face of the sample chamber. The hexagonal wheel permitted each sample to be rotated into measurement position. The remaining five samples in the chamber were completely masked off from a direct view of either the source or detector. A black matte liner on all inside surfaces of the chamber served to reduce light scattering, and a light baffle was built in to block the direct line of sight between source and detector.

The two types of measurement geometries are illustrated in Figures 1 and 2. In both geometries the illumination and detection angles are 60 degrees to the sample surface normal. In the Type I geometry (Figure 1) a 10 x 15 mm sample surface area is illuminated with focused, monochromatic light. The sample surface is viewed by the detector through a circular aperture of 3.6 cm diameter at a centerline distance of



GEOMETRY FOR TYPE I MEASUREMENTS

FIGURE 1.



GEOMETRY FOR TYPE II MEASUREMENTS

FIGURE 2.

7.4 cm between sample and detector. Because of the broad spectral sensitivity of the detector, the recorded signal in this case includes both the sample reflectance at the incident monochromatic wavelength and any ultraviolet or visible (up to about 6000Å) luminescence which the incident wavelength excites.

In the type II geometry (Figure 2) the entire sample surface is illuminated with the full hydrogen source spectrum. The sample reflectance plus luminescence is then detected with spectral selectivity through the monochromator. The monochromator field of view covers a sample surface area of about 14 mm x 10 mm. Each element within this surface area, however, is detected with a very small acceptance angle defined by the entrance slit of the monochromator (0.3 mm x 10 mm) at a center line distance of 8.4 cm between sample and slit.

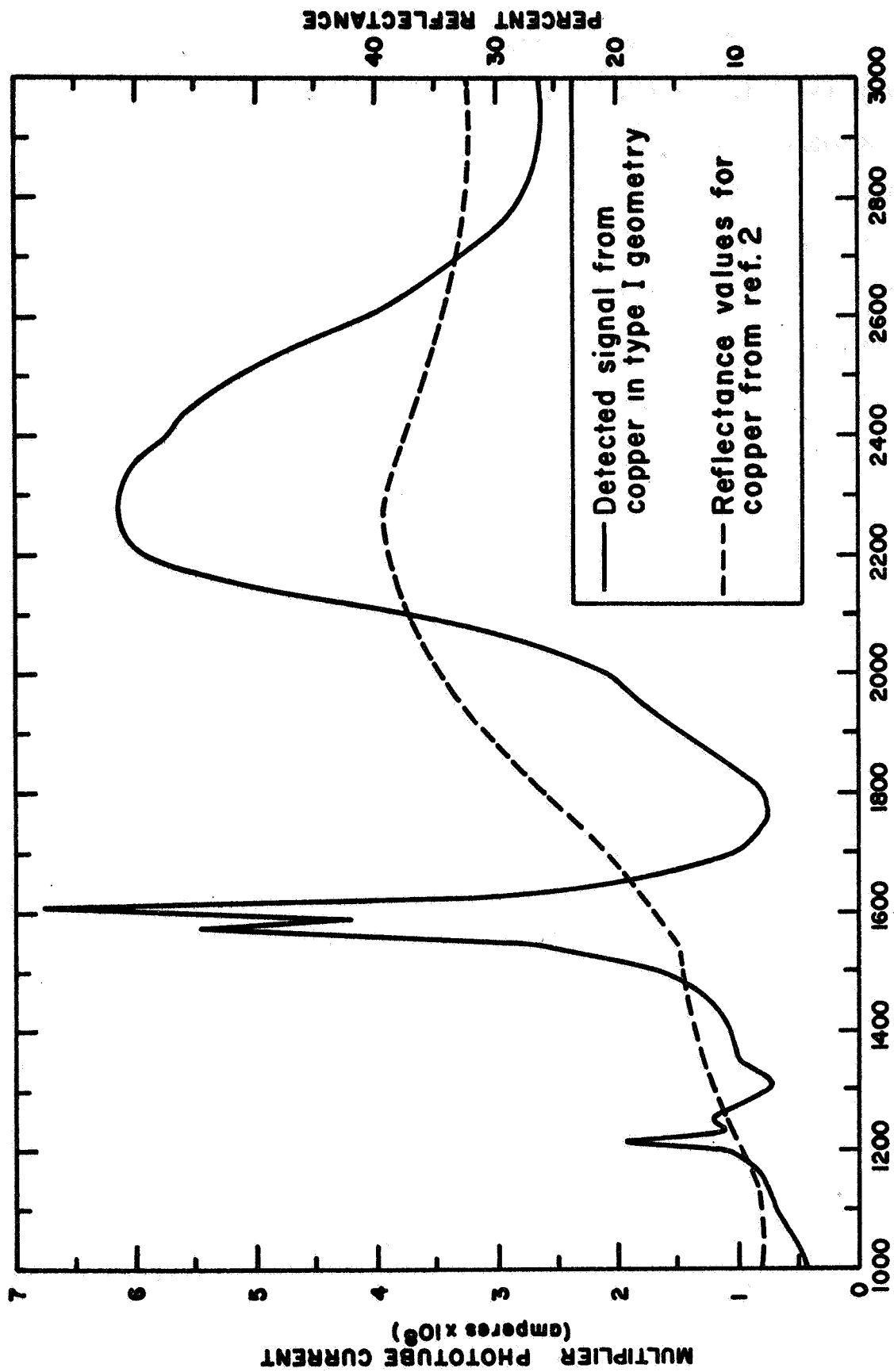
#### D. Measurement Methods and Standardization

The sample chamber was loaded with either five or four samples and one or two reference materials for each set of measurements. The entire unit, monochromator and sample chamber, was pumped down to  $10^{-5}$  mm or less pressure and outgassed for at least two hours before the hydrogen gas flow to the source was begun. When a stable hydrogen gas flow had been reached (with the hydrogen flow the monochromator pressure is about  $10^{-3}$  mm), the source is ignited and allowed to stabilize. In the type II

geometry, where the sample chamber is between the source and the monochromator, some differential pumping is used between the source and samples to reduce the hydrogen content at the samples.

Most of the data were obtained by recording the detector signal as the monochromator was scanned from 3000A down to 1000A at a scan rate of 100A per minute. In all cases a reference piece of polished aluminum was in the sample chamber and was scanned intermittently between sample scans. The signal data for the sample scans were then normalized to the aluminum reference signal at the corresponding wavelengths. The function of the aluminum reference was primarily to monitor the source output. Absolute reflectance values were eventually derived on the basis of a polished copper piece which was compared to the aluminum reference. The values of Ehrenreich and Phillipp (Ref. 2) for the absolute reflectance of polished bulk copper in the vacuum ultraviolet were used to calibrate the aluminum reference.

The detected signal (multiplier phototube current) versus wavelength from the polished copper reference in Type I geometry is shown in Figure 3. Also plotted in this figure is the copper spectral reflectance curve which was used as the standard. The detected signal curve shape is a function of the hydrogen source spectrum, the detector spectral response, and the sample reflectance. Two features of the hydrogen source are prominent on all of the raw data curves; these are the hydrogen Lyman line at 1215A and the high intensity peaks around 1600A.



COPPER REFERENCE DATA

FIGURE 3.



The final standardization of the reflectance values was confused at first when a comparison of the aluminum reference and the copper standard gave relative values which were not compatible with their literature values. Further experiments utilizing fresh aluminum and copper samples were then performed to establish the correct reflectance value standard. These experiments were successful in explaining the early discrepancy as being due to a degradation of the aluminum reference sample reflectance caused by the hard ultraviolet radiation. Fortunately, the original aluminum reference had been degraded during the very first checkout runs prior to the sample data runs so that the aluminum remained as a constant secondary reference to which the copper standard could be correlated.

To verify the reproducibility of test results, data on three samples were taken twice by scanning runs on separate days and once at fixed wavelength points, where the wavelength was held constant while the detected signals were measured alternately from the samples and from reference materials in the chamber. The final curves derived from these samples had essentially the same shapes for each of the three measurements.

### III. DATA AND DISCUSSION

In Table 1 the eight rocks are listed in order of the generally expected decreasing silica content, from the acidic biotite granite and rhyolite to the ultra-basic dunite. Detailed compositional and surface texture analyses have not been performed; however, these samples are available if such studies are warranted.

The normalized data curves obtained for both Type I and Type II geometries of the same sample surface are presented in the Appendix. Data points were analyzed and plotted at 50 Angstrom intervals except for wavelengths near 1200 A and 1600 A where the source input maxima produced such sharp slopes in signal change on the recorded scans (see, for example, Figure 3), that it was not possible to obtain a precise data point.

To determine the fraction of energy collected at the detector from the total emission reflection by the rock surface, the detector solid angle was computed and compared

to the total angle of emission or reflection. The estimated fractions from Figures 1 and 2 are specified below:

- a) Type I, diffuse reflectance -- 0.06
- b) Type I, luminescence emission -- 0.03
- c) Type II, diffuse reflectance --  $2 \times 10^{-4}$
- d) Type II, luminescence emission --  $1 \times 10^{-4}$

In both geometries the sample surface normal was adjusted and fixed so that the source and detector angles to the normal satisfied the law of specular reflection; this was observed by a peaking of the response of the detector. Thus the detection fractions for the specularly reflected components are assumed to be unity for both geometries.

Using the above detection fractions we can write the equations for the relative components of the detected signals. No specular reflectance component is included in the "ground" surface measurements equations.\* The signal equations are written below with the designations (P-I), (P-II), (G-I), and (G-II) wherein the symbols P and G refer to the polished and ground surfaces, and the symbols I and II refer to the measurement geometries.

$$(P-I)_{\lambda} = R_s(\lambda) + 0.06 R_d(\lambda) + 0.03 L_I \quad (1)$$

$$(P-II)_{\lambda} = R_s(\lambda) + 2 \times 10^{-4} R_d(\lambda) + 10^{-4} L_{II} \quad (2)$$

---

\* The data of Reference 1 showed no significant differences in ground surface reflectance curves with or without the inclusion of the specular reflectance component.

$$(G-I)_{\lambda} = 0.06 R_d^1(\lambda) + 0.03 L_I \quad (3)$$

$$(G-II)_{\lambda} = 2 \times 10^{-4} R_d^1(\lambda) + 10^{-4} L_{II} \quad (4)$$

where:

$R_s(\lambda)$  = specular reflectance at wavelength  $\lambda$ ,

$R_d(\lambda)$  = diffuse reflectance at wavelength  $\lambda$ , from the polished surface,

$R_d^1(\lambda)$  = diffuse reflectance at wavelength  $\lambda$ , from the ground surface,

$L_I$  = luminescence excited by narrow band (5A) energy increment at  $\lambda$  and detected with broad band detector, and

$L_{II}$  = luminescence excited by direct broad band source and detected with narrow band (5A) resolution at  $\lambda$ .

The  $L_I$  signal component as a function of wavelength is the luminescence excitation spectrum. In general for mineral or inorganic luminescent materials, the excitation spectra will have a threshold and then increase as the wavelength decreases to a nearly constant efficiency over a broad range of wavelengths.

The  $L_{II}$  signal component as a function of wavelength is the luminescence emission spectrum. Luminescence emission will occur at longer wavelengths than the excitation wavelength. In a simple luminescent system the emission spectrum is a band with a width at half maximum intensity of several hundred Angstroms. Materials such as rocks may

have several overlapping emission bands and a very broad and/or complex spectrum.

Examination of the components contributing to the normalized measured quantities (left-hand sides of Equations 1-4), leads to the following:

1. The extremely small coefficients modifying the diffuse ( $R_d$ ) and luminescence ( $L_{II}$ ) contributions to the (P-II) measurements, Equation 2, tend to remove these contributions in this measurement. Therefore, it is highly likely that the (P-II) curves shown in the Appendix exhibit predominantly the specular reflectance properties of the polished rock samples.
2. The (G-II) data curves are the most favorable sources of information for detecting luminescence. The ground-surface measurements, Equations 3 and 4, remove a major contribution from specular reflection, in contrast to those from the polished surface, Equations 1 and 2. Thus, the ground-surface measurements leave only the diffuse reflection component to compete with the luminescence emission in data interpretation. A comparison of the  $L_I$  and  $L_{II}$  intensities can be deduced directly from Equations 3 and 4; the effects of differing source intensities employed in the two geometries have been removed in these equations by normalization of the (G-I) and (G-II) values measured.

Solving Equations 3 and 4 simultaneously to remove the diffuse reflectance contributor,  $R_d^1$ , one obtains,

$$L_{II} - L_I = 10^4 (G-II)_\lambda - 33 (G-I)_\lambda \quad (5)$$

For all rock samples investigated, the normalized data values

indicate that,

$$(G-I)_{\lambda} \leq 43(G-II)_{\lambda} \quad (6)$$

So that, in all cases  $L_{II}$  is greater than  $L_I$  and therefore,

$$\frac{L_{II}}{R_d^I} > \frac{L_I}{R_d^I} \quad (7)$$

which indicates the advantage of the (G-II) data curves over the (G-I) data for detection of luminescence. The Appendix curves for the ground surfaces tend to corroborate this since the Type II geometry data exhibits considerably more peaking than does the Type I data. Such peaking has been interpreted as probable evidence of luminescence.

Polished Surface - Type I Geometry: 1000-1800 A, a large continuous increase in value with inflections around 1400 and 1600; 1800-2000 A, a broad maximum; 2000-3000 A, a moderate continuous decrease in value.

Ground Surface - Type I Geometry: 1000-2000 A; similar to Polished - Type II; 2000-3000 A values increase with gradual slope (essentially an inversion of Polished - Type II behavior).

Ground Surface - Type II Geometry: Note that these signals are relatively low and subject to larger errors in data points. There is a resolved maximum peak at 2400 A in all samples and a secondary maximum around 1800 A. An inflection or peaking at 2050 is also indicated. Any structure in curve shape below 1700 is questionable.

2. Group 2 - Monzonite, diorite, obsidian

Polished Surface - Type II Geometry: 1000-2050 A, continuously increasing values rising to a sharp peak at 2050; 2050-3000, same as Group I.

Polished Surface - Type I Geometry: 1000-1800 A, a very pronounced maximum peak about 1650; 1800-3000 A, same as Group 1.

Ground Surface - Type I Geometry: generally similar to Group 1 except for obsidian whose value stays about constant from 1800-3000 A.

Ground Surface - Type II Geometry: monzonite and diorite have their maximum peak at 2050 with an indication of

a secondary peak around 2400. Obsidian's curve shape is similar to Group 1, in contrast to its polished surface behavior.

3. Rhyolite and Gabbro

Polished Surface - Type II Geometry: rhyolite tends toward Group 2 shape while gabbro tends toward Group 1 shape.

Polished Surface - Type I Geometry: Both samples look most similar to Group 2 curves.

Ground Surface - Type I Geometry: similar to Group 1 shape rhyolite has a sharp break at 2400 with a very strong increase up to 3000.

Ground Surface - Type II Geometry: same as Group 1 curves.

4. Pumice

Type I Geometry: generally similar curves to Group 1.

Type II Geometry: the pumice surface number 3 (see curve (1, 3) fits the Group 1 curve shape; pumice surface number 2, however, has an anomalous shape intermediate to the two basic groups.

5. Meteorites - Hypersthene Chondrite and Coarse Octahedrite

As mentioned earlier these samples had surfaces different from the rocks. Also the measurements were only performed in the point by point technique at 100 A intervals.

Hypersthene Chondrite (mottled surface): Type I geometry between 1000-2600 A appears similar to Group 1 - ground



surface data with a sharp increase around 1800; 2600-3000, values decrease similar to polished surface rock data. Type II geometry curve is unique with a broad maximum peaking at 2300 A.

Coarse Octahedrite (high metal-like polish): Type I geometry curve appears like a polished metal reflectance curve, note the high reflectance values. Type II geometry curve does indicate some possible structure, more data points would be necessary to confirm this.

#### IV. OBSERVATIONS

1. All samples, both ground and polished surfaces, have increasing reflectance values as the wavelength increases between 1000 A to 2000 A. The predominant increase occurs between 1600 A and 2000 A.
2. As the wavelength increases from 2000 A to 3000 A, the spectral reflectance decreases for polished surfaces and increases for ground surfaces. The largest relative differences in slope values of the curves occur for the ground surfaces.
3. The gross aspects of the ground surfaces are similar in that one or more relatively sharp peaks and changes in slope direction are common for all ground surfaces. Fewer sharp peaks and changes in slope are noted for the polished surfaces. These and other similarities in gross aspects of the curves suggest that surface texture rather than composition are major factors in determining spectral reflectance, particularly at wavelengths shorter than 2000 A.
4. The general curve characteristics for monzonite and diorite are markedly similar to each other, and likewise, markedly dissimilar to rocks of more acidic and basic composition. However, curve characteristics of other rock types bear no relation to composition. For example, curves for polished biotite granite are more similar to curves for dunite, an ultrabasic rock unrelated compositionally, than they are to rhyolite which is compositionally similar to granite.

5. All rocks showed a luminescence emission at about 2400 A, while monzonite and diorite had their peak emission at 2050 A. The high source intensity around 1600 A was distinctly exciting luminescence, but without a correlation with the emission bands it is not possible to estimate the observable emission under solar illumination.

V. CONCLUSIONS AND PLANS FOR FUTURE WORK

Although initial analyses of monzonite and diorite at wavelengths shorter than 3000 Å suggest a correlation between composition and UV spectral response, other rock samples of more acidic and basic composition displayed little or no correspondence with their spectral reflectance curves. Quite possibly this lack of correspondence is due to differences in surface texture between the sample surfaces. Although identical abrasives were used to prepare all sample surfaces, it is possible that the standard rock polishing methods used are inadequate, especially at wavelengths shorter than 2000 Å where irregularities in the surface may be comparatively large with respect to wavelength.

It is also possible that surface preparation of the samples may somehow modify the molecular structure of the surface layer so that the emission spectrum is altered or quenched. It would be desirable in future work to include several samples ranging from highly polished to finely powdered ( $\sim 50$  Å), prepared from the same specimen, in order that the effect of surface texture on both reflectance and emission may be studied.

## REFERENCES

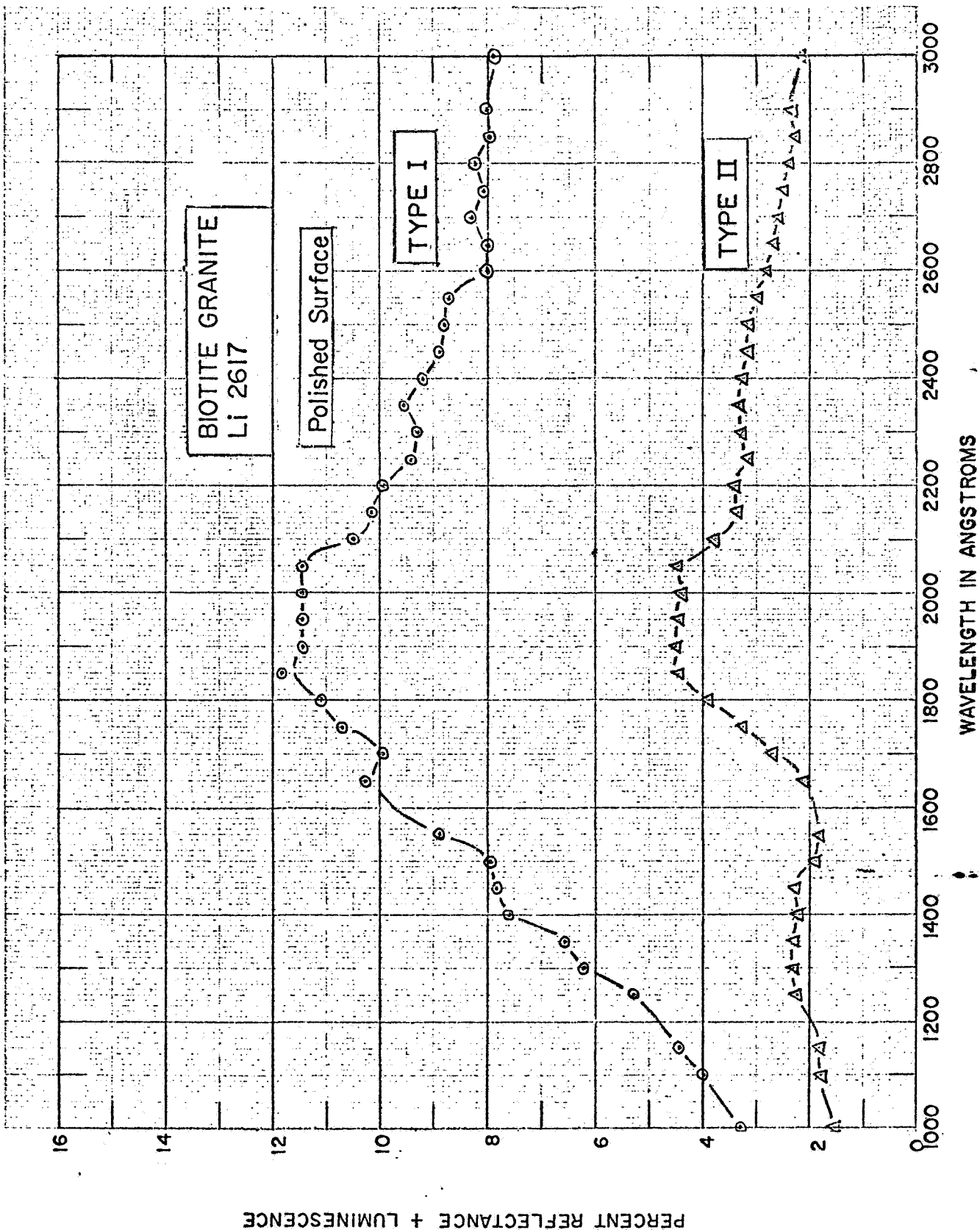
1. H. V. Watts, "Reflectance of Rocks and Minerals to Visible and Ultraviolet Radiation", Technical Letter NASA-32, July 1966.
2. H. Ehrenreich and H. R. Phillipp, "Optical Properties of Ag and Cu", Phys. Rev. 128, No. 4, 1622 (1962).
3. A. N. Thorpe, C. M. Alexander, and F. E. Senftle, "Preliminary Ultraviolet Reflectance of Some Rocks and Minerals from 2000 A to 3000 A", Technical Letter NASA-37, August 1966.
4. Norman N. Greenman, et. al., "Feasibility Study of the Ultraviolet Spectral Analysis of the Lunar Surface", Douglas Report SM-48529, March 1965.

## APPENDIX

### DATA CURVES

APPENDIX  
Table of Contents

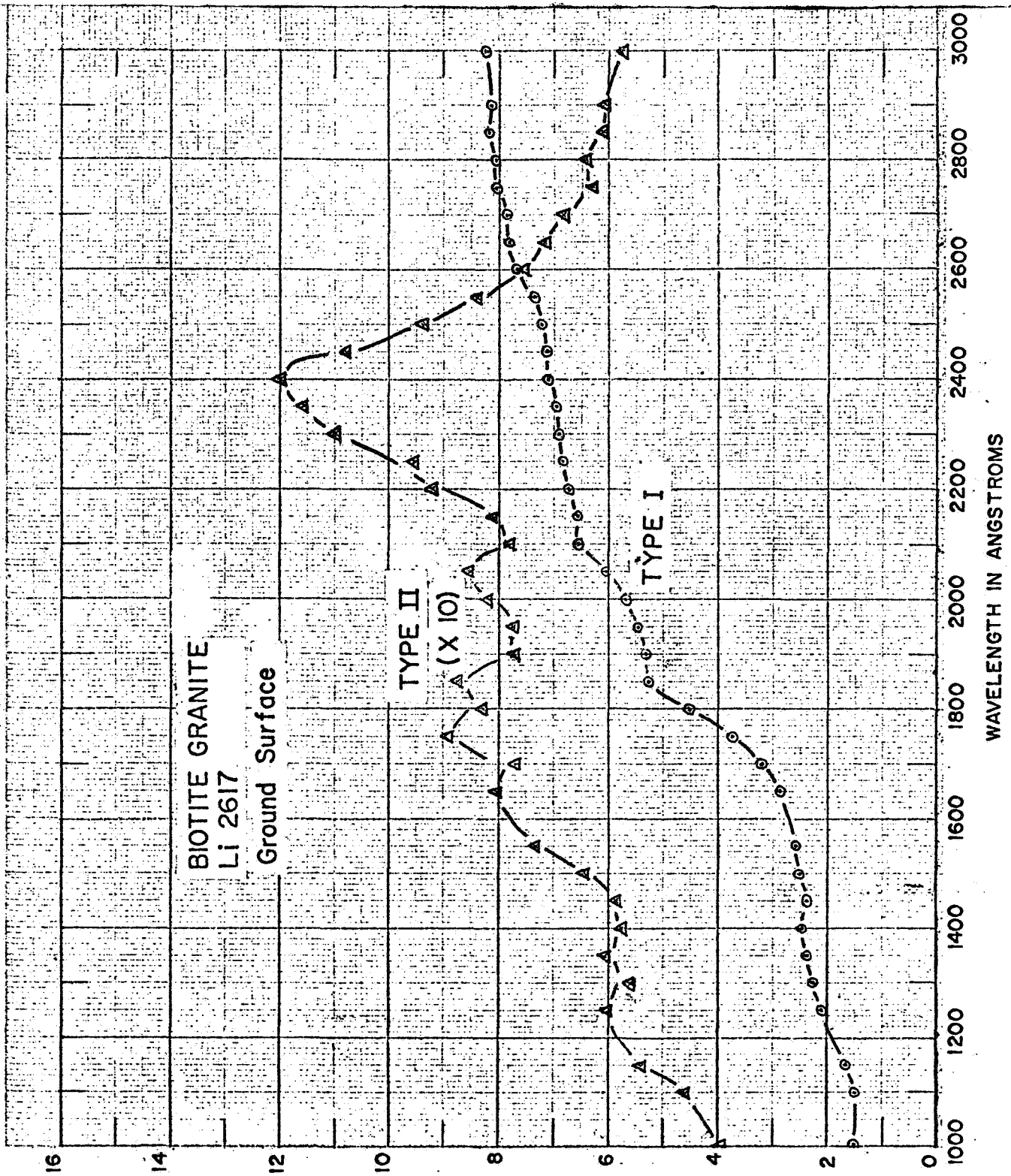
	<u>Page</u>
<u>DATA CURVES:</u>	
Biotite granite, polished	A-1
ground	A-2
Rhyolite, polished	A-3
ground	A-4
Monzonite, polished	A-5
ground	A-6
Diorite, polished	A-7
ground	A-8
Gabbro, polished	A-9
ground	A-10
Basalt, polished	A-11
ground	A-12
Dunite, polished	A-13
ground	A-14
Obsidian, polished	A-15
ground	A-16
Pumice, (designated 1, 3)	A-17
Pumice, (designated 2, 2)	A-18
Hypersthene chondrite, mottled surface	A-19
Coarse octahedrite, high polished surface	A-20

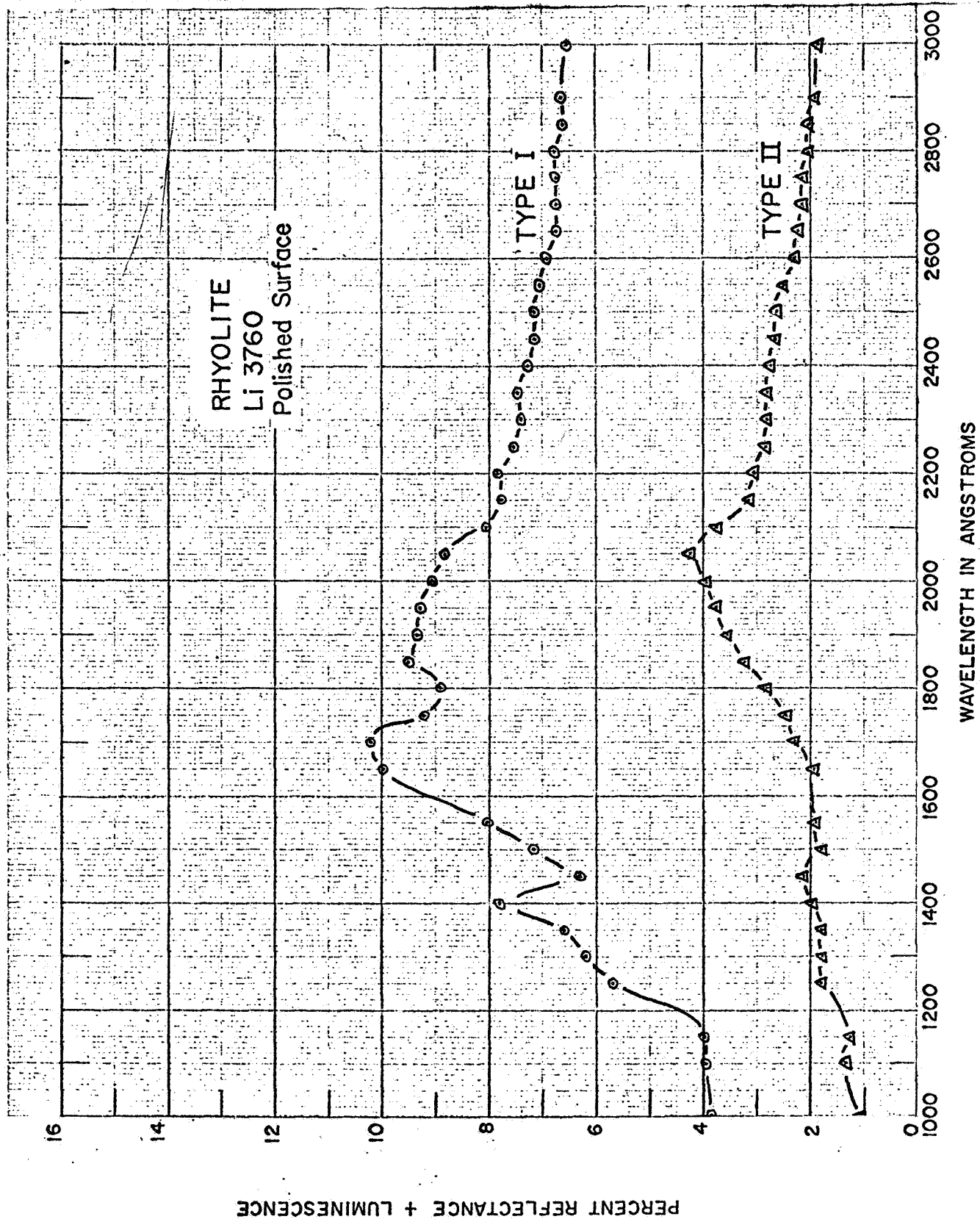




PERCENT REFLECTANCE + LUMINESCENCE

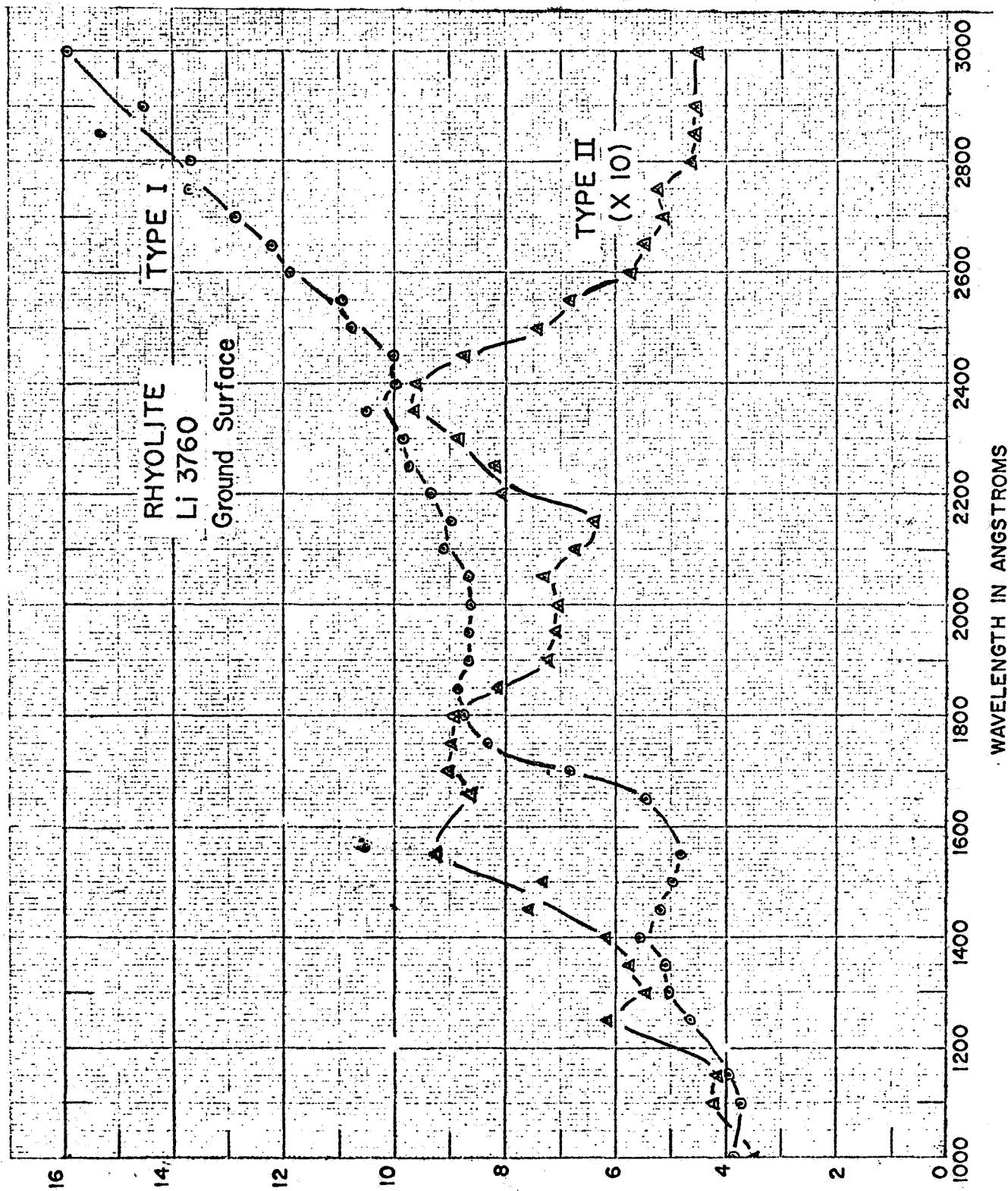
A-2

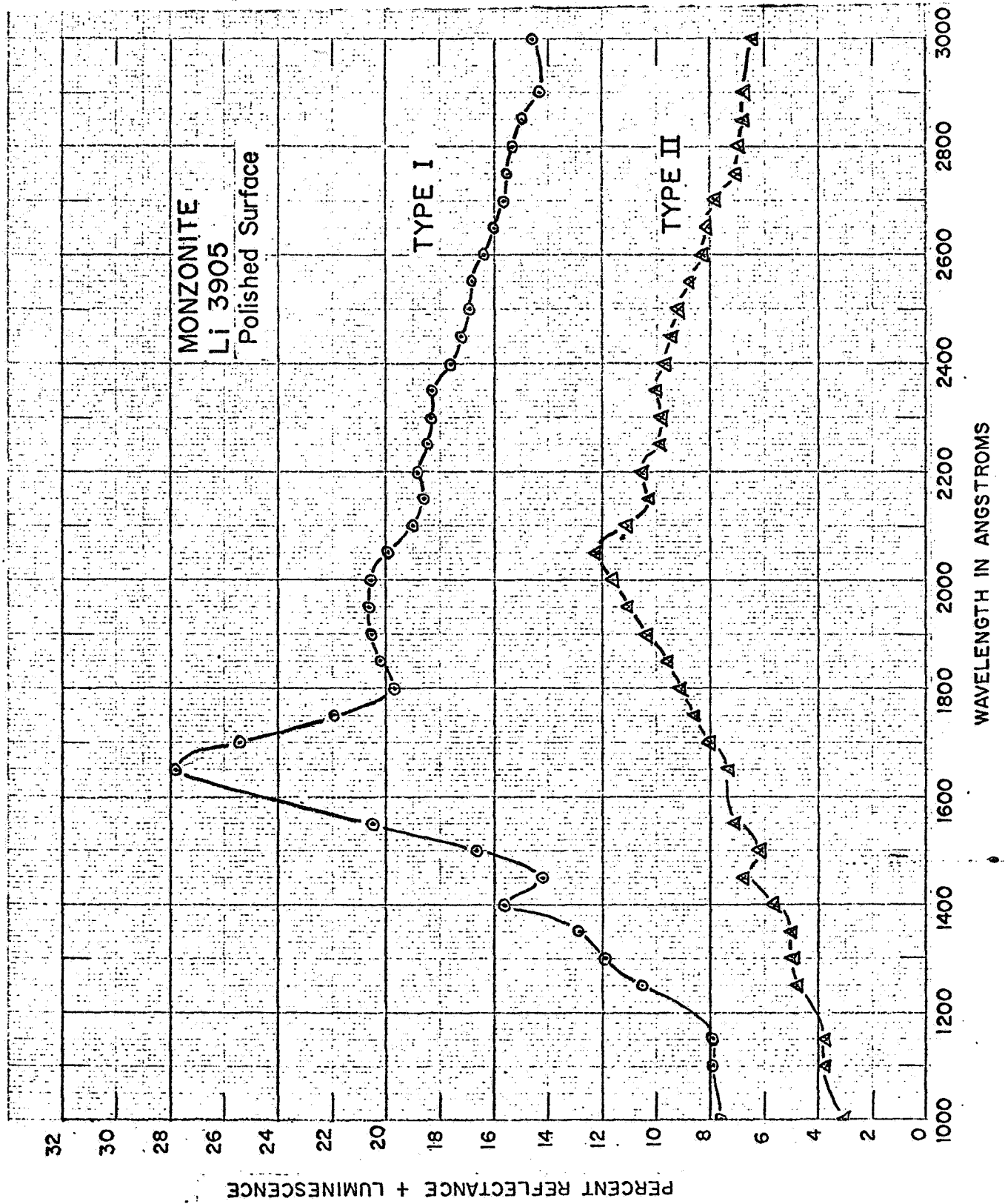


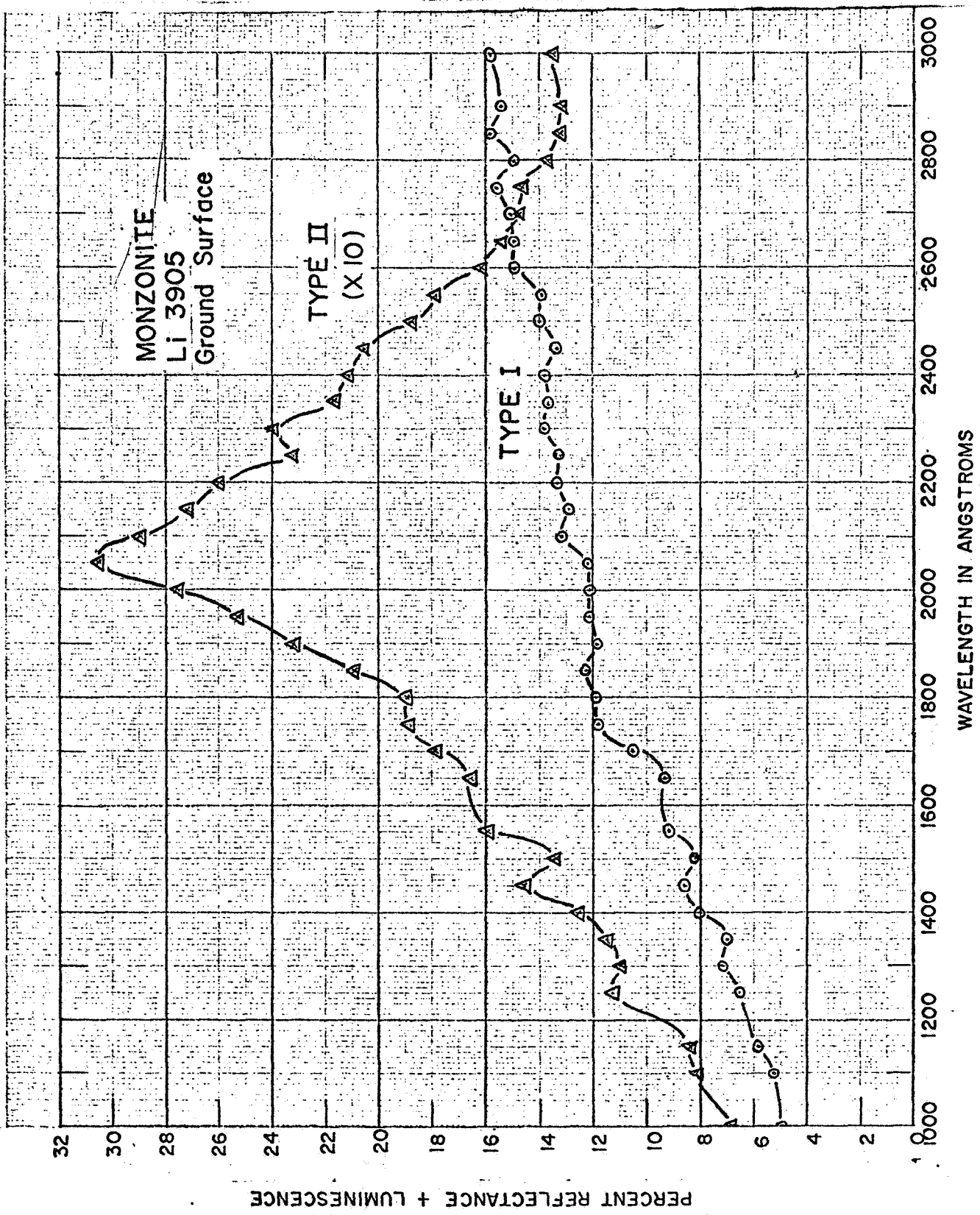


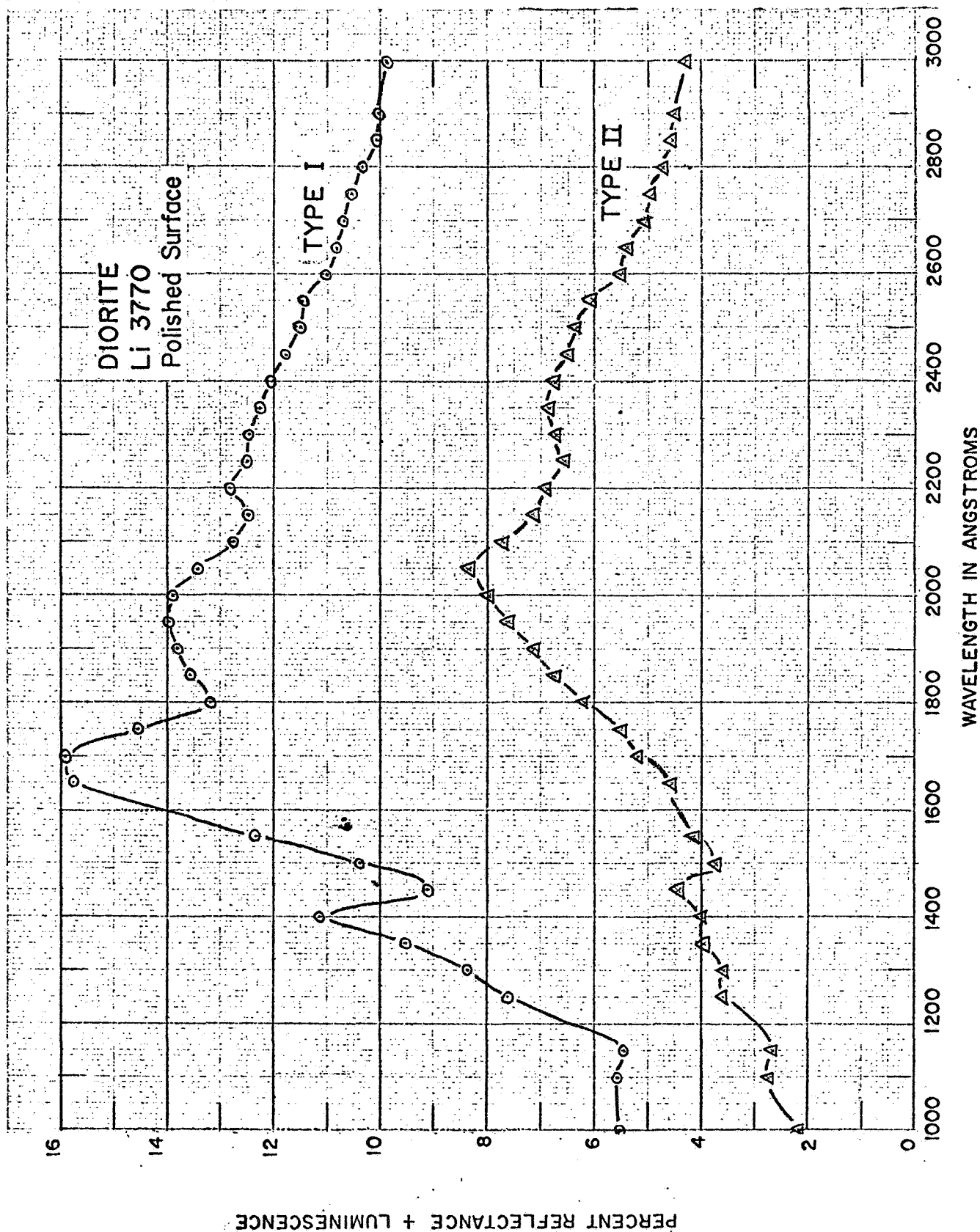
PERCENT REFLECTANCE + LUMINESCENCE

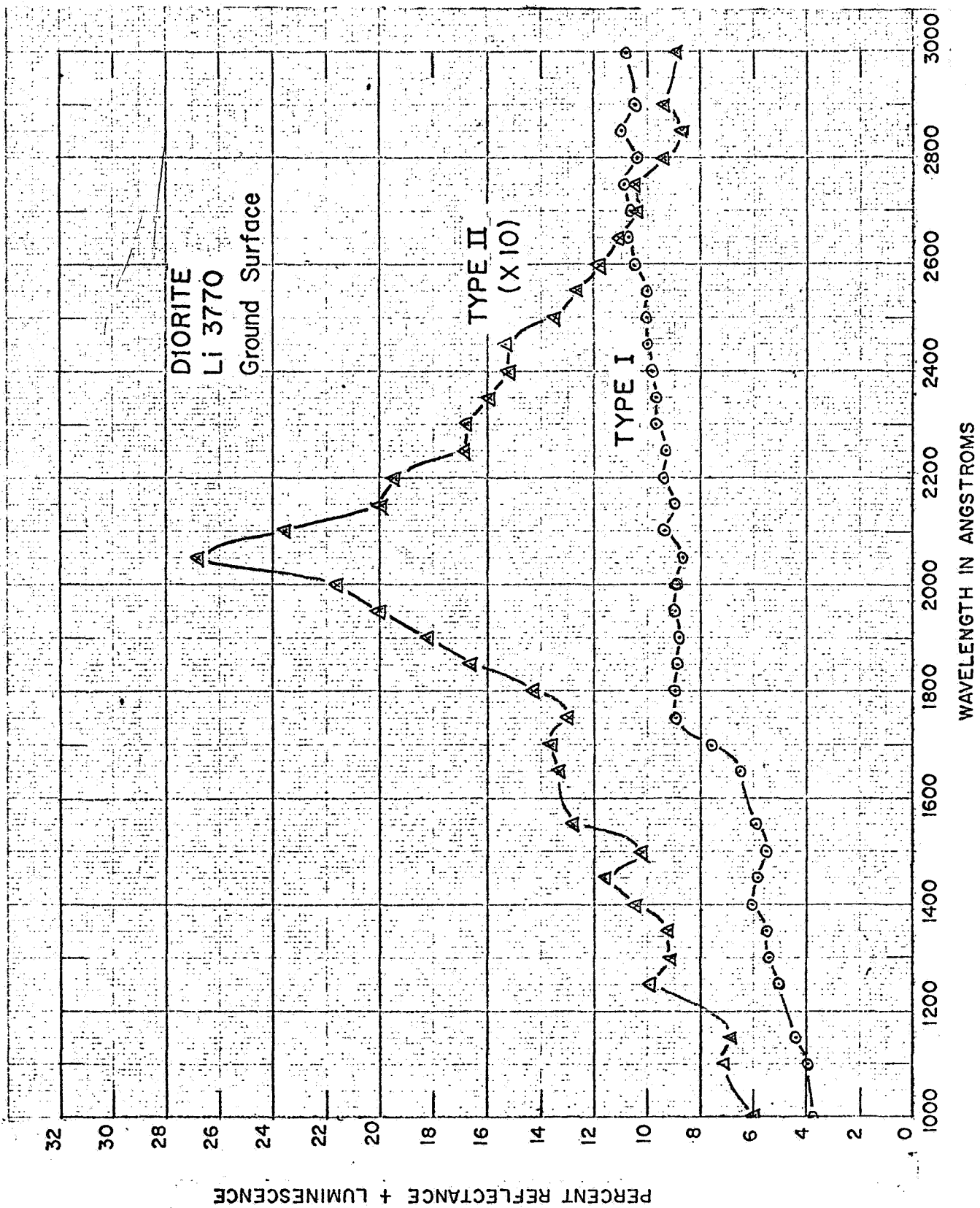
A-4

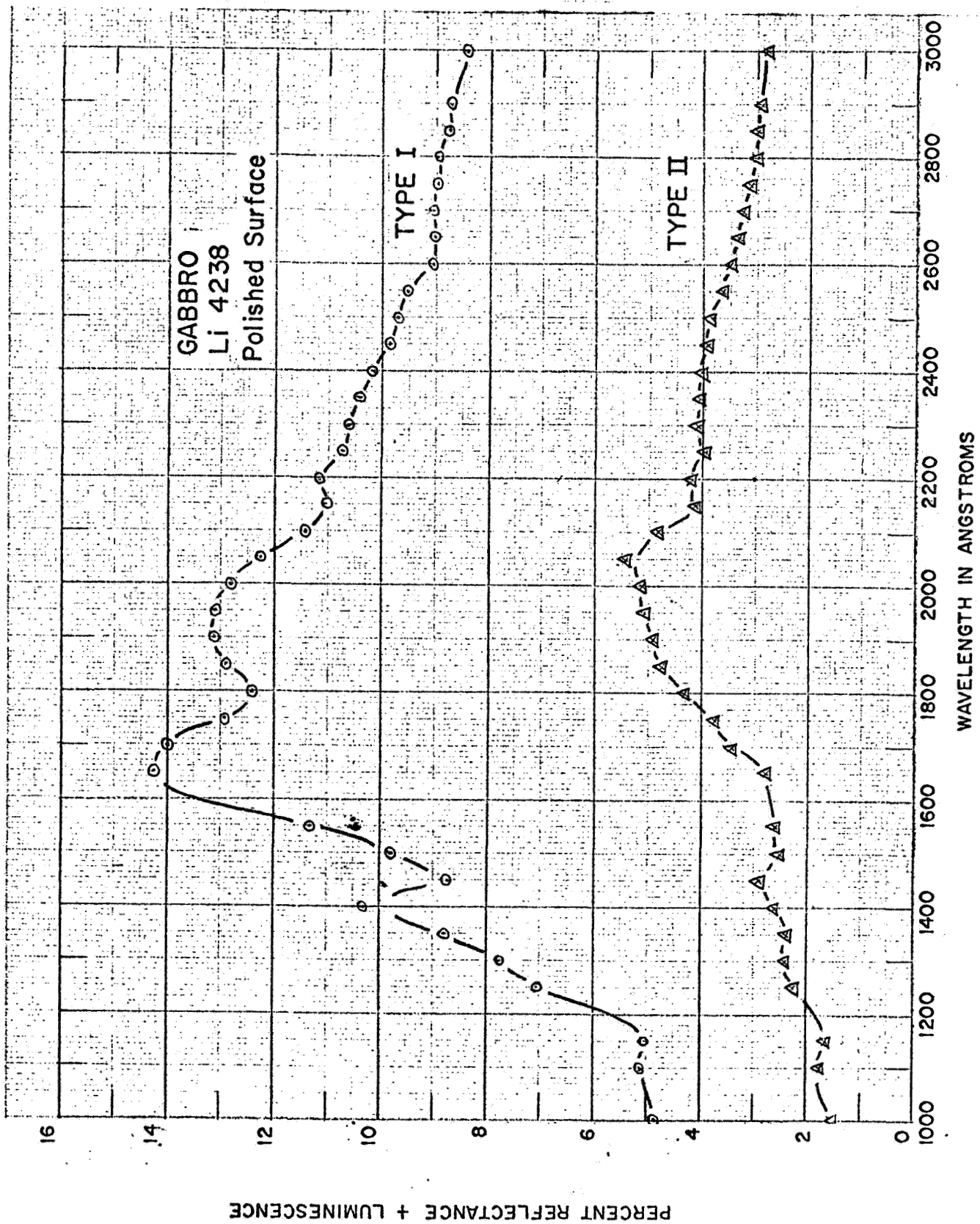




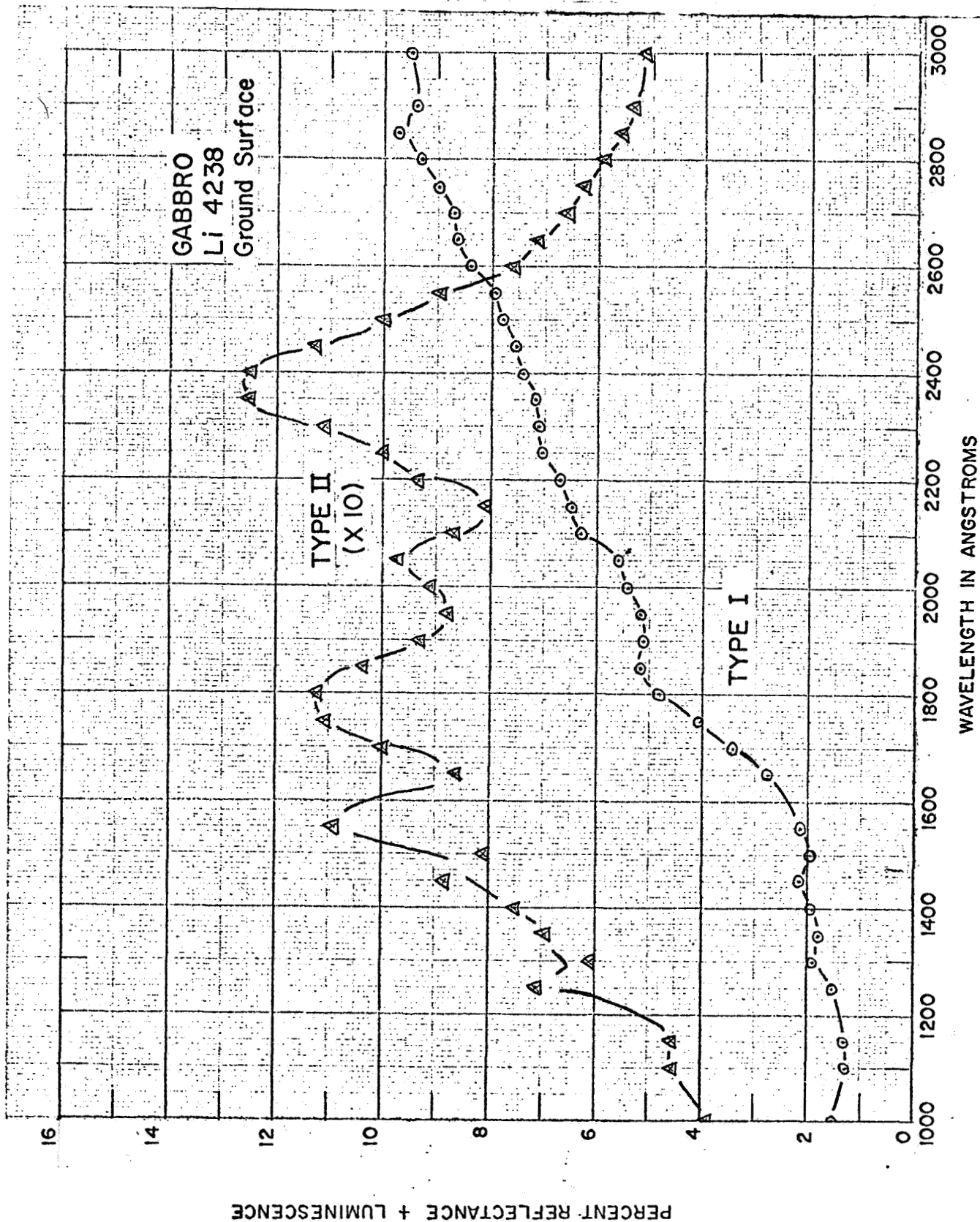


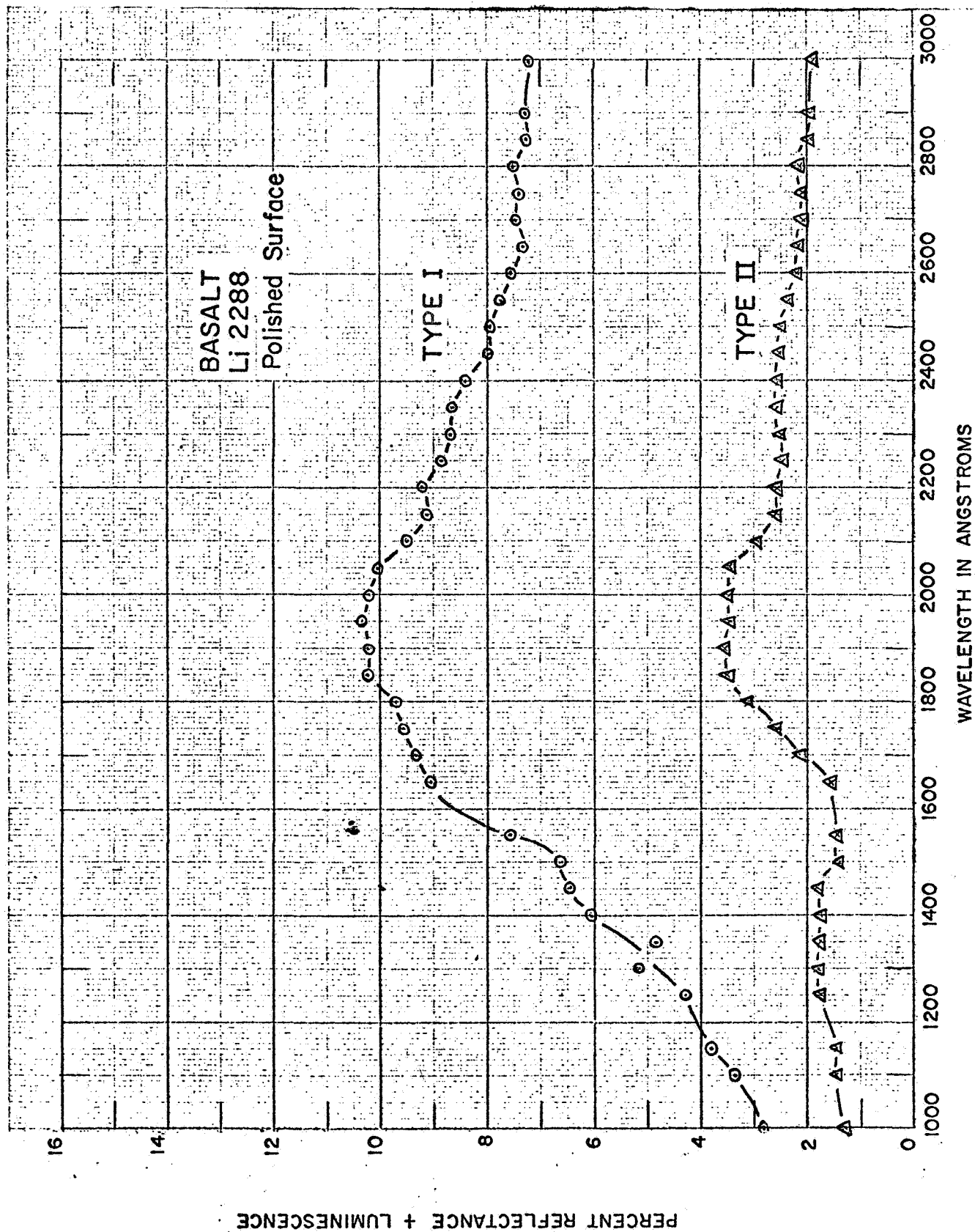


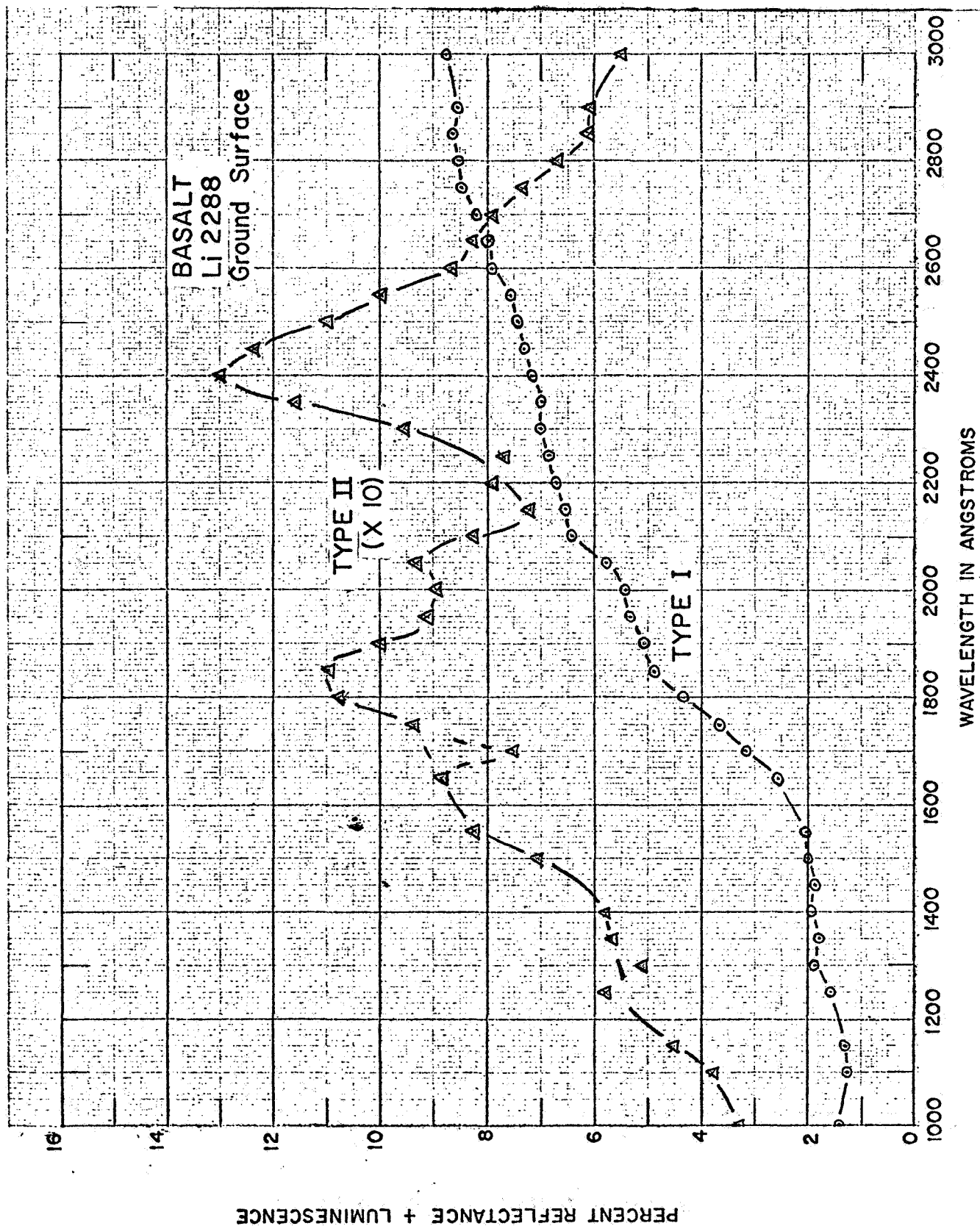


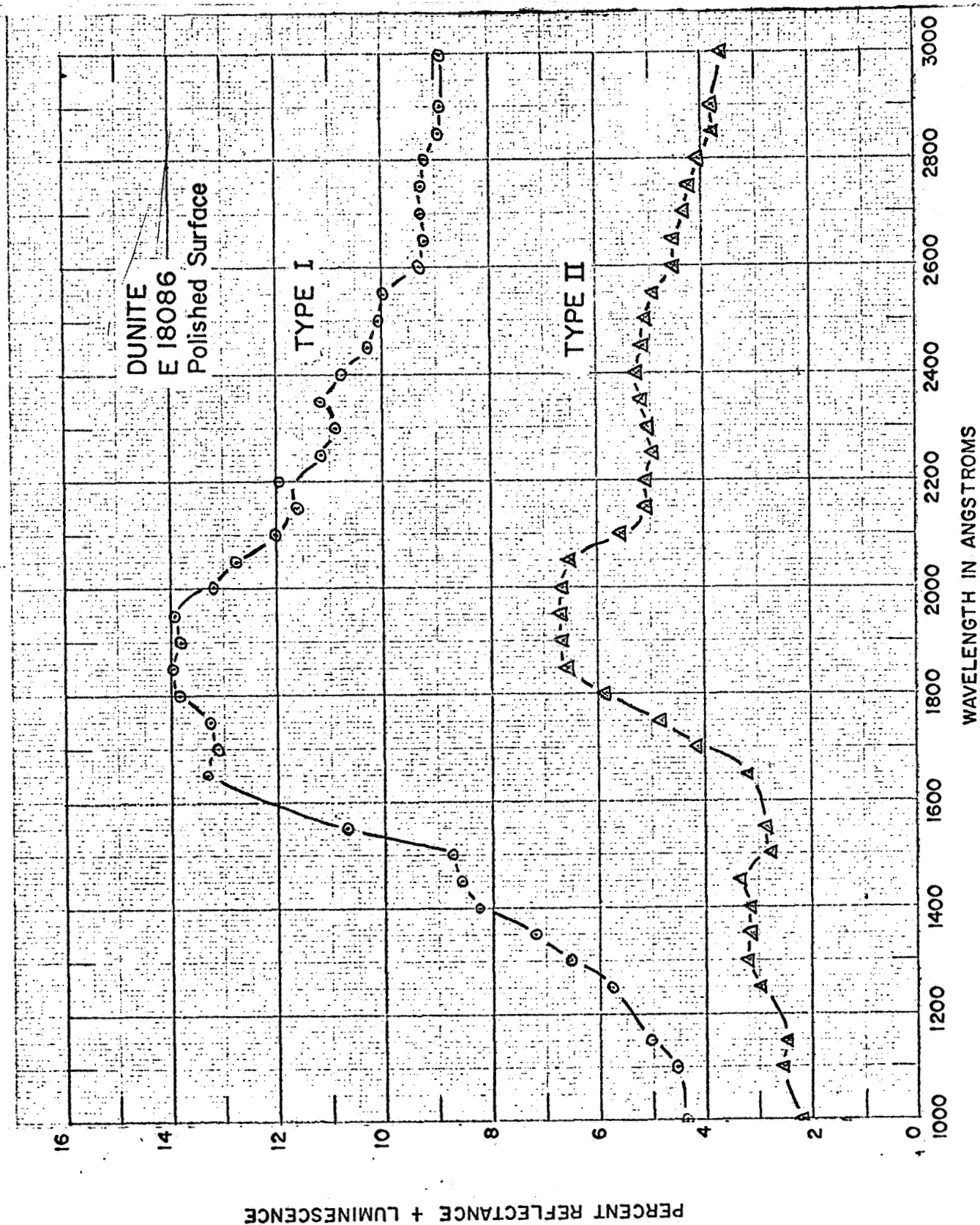


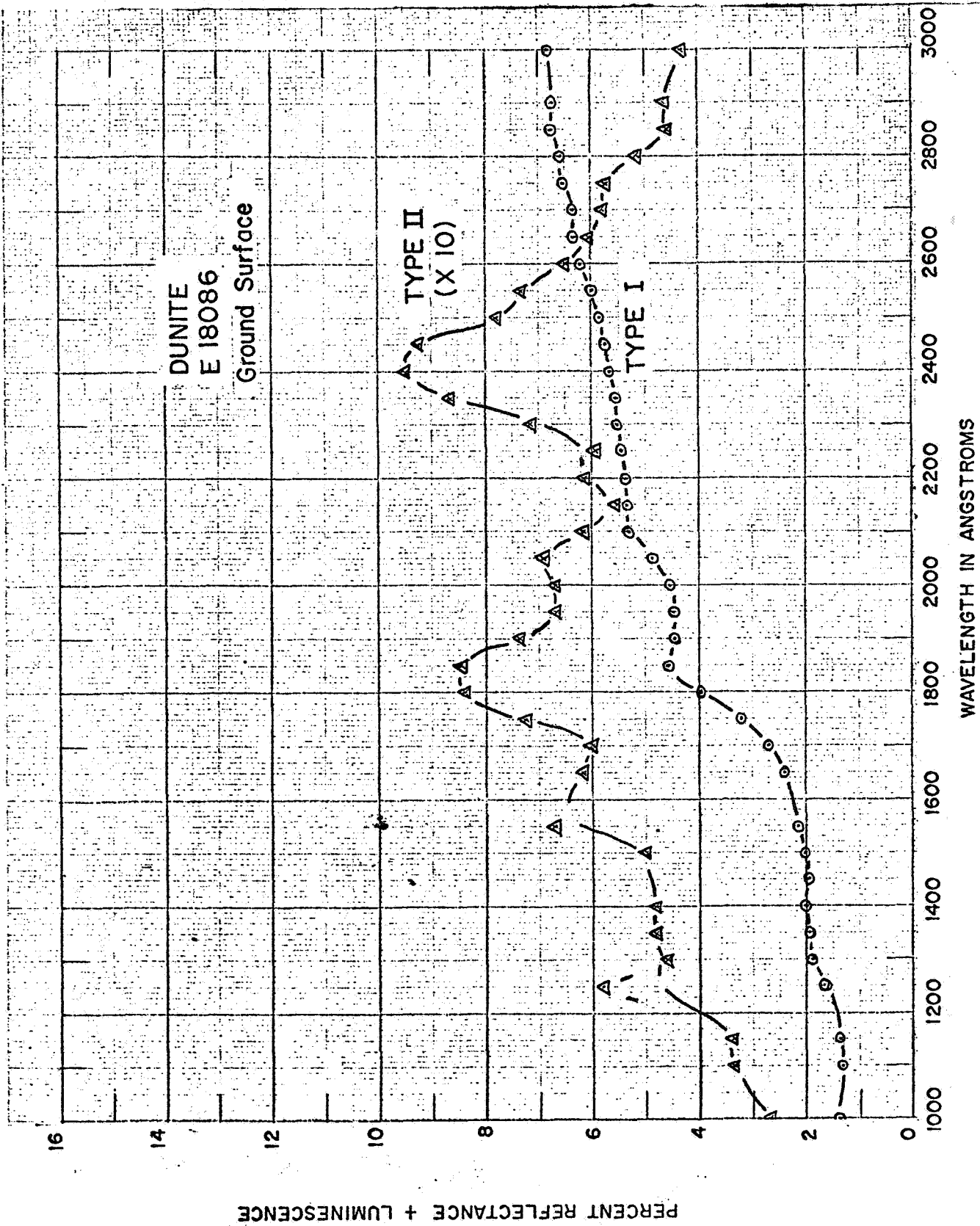


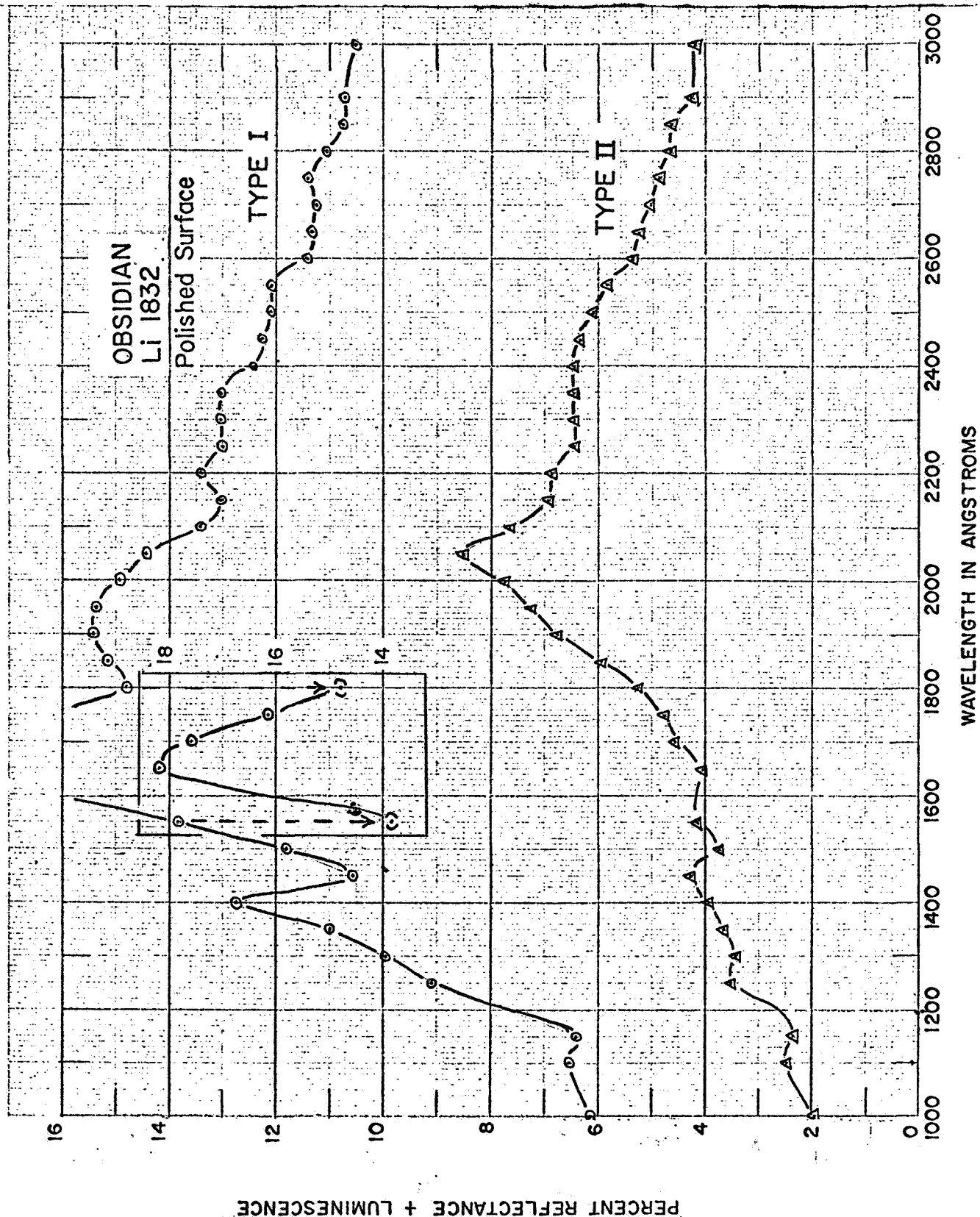


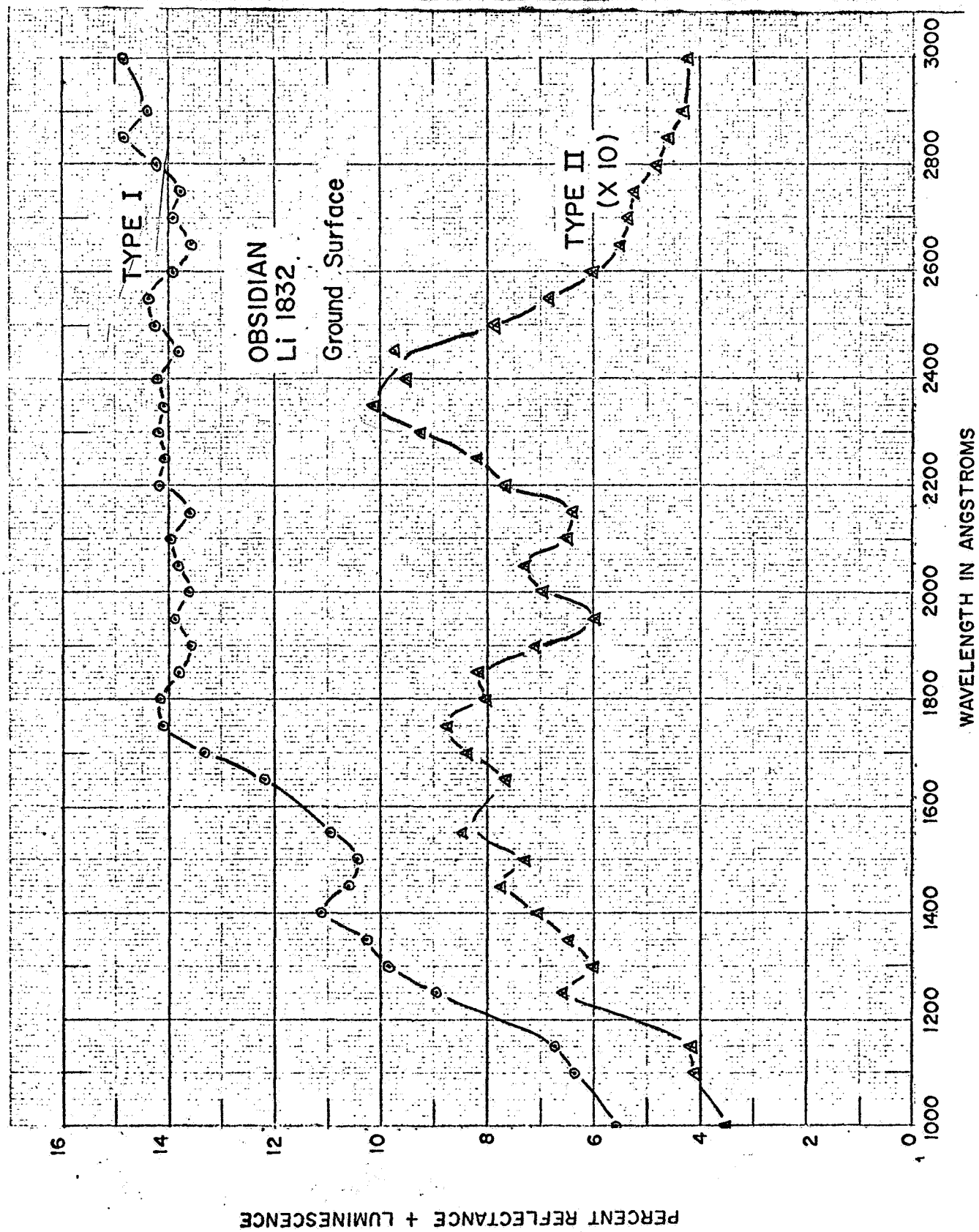




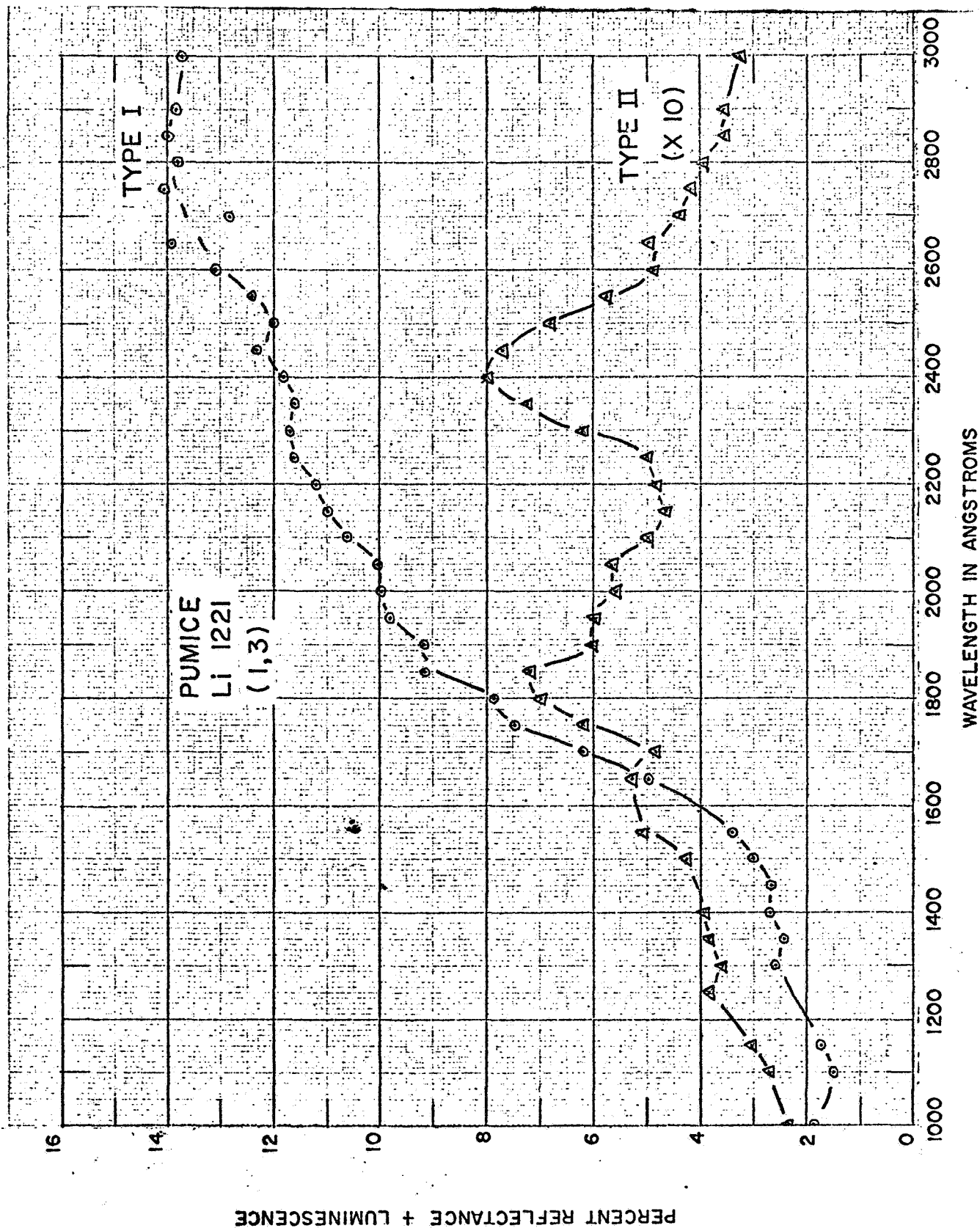








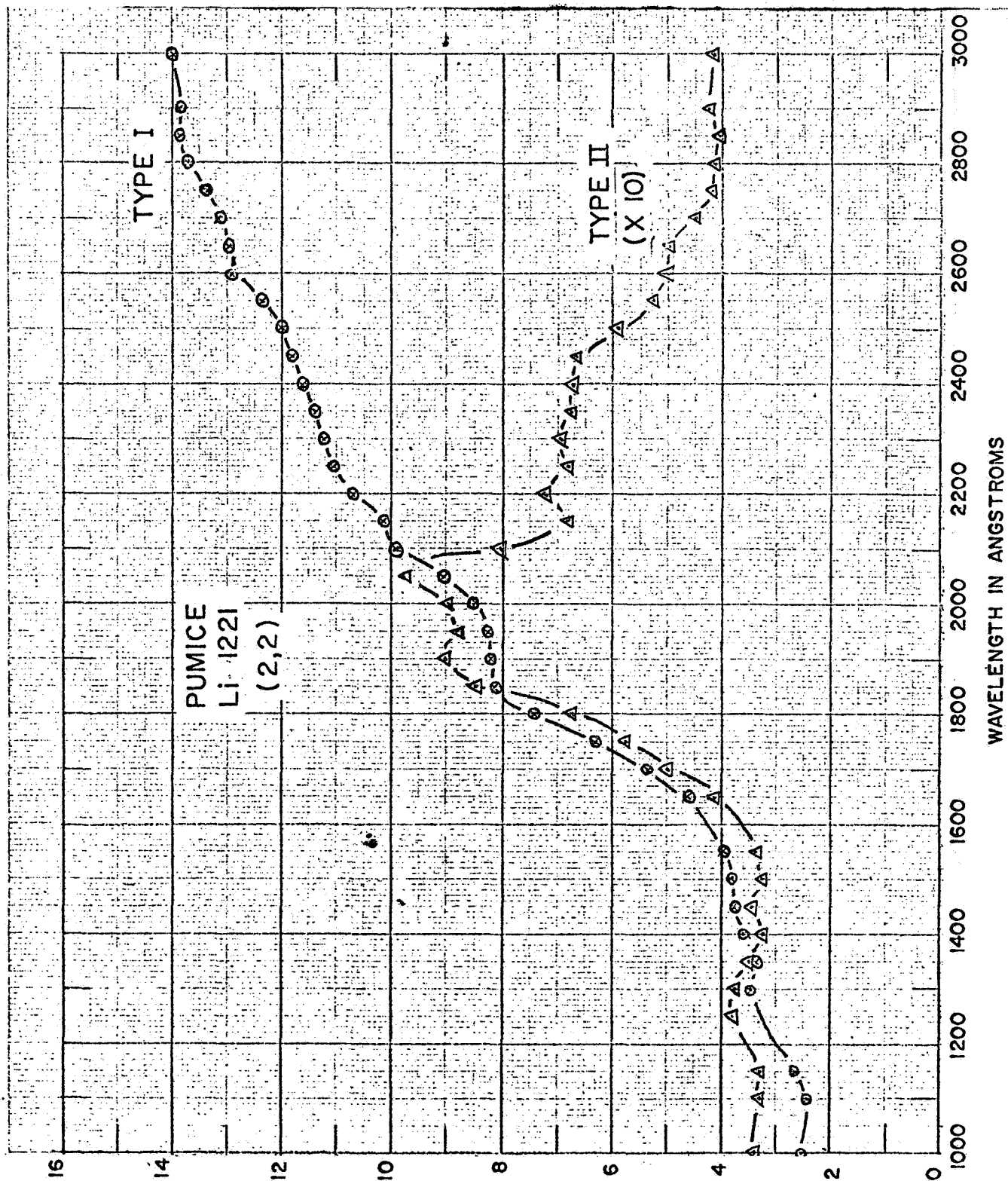




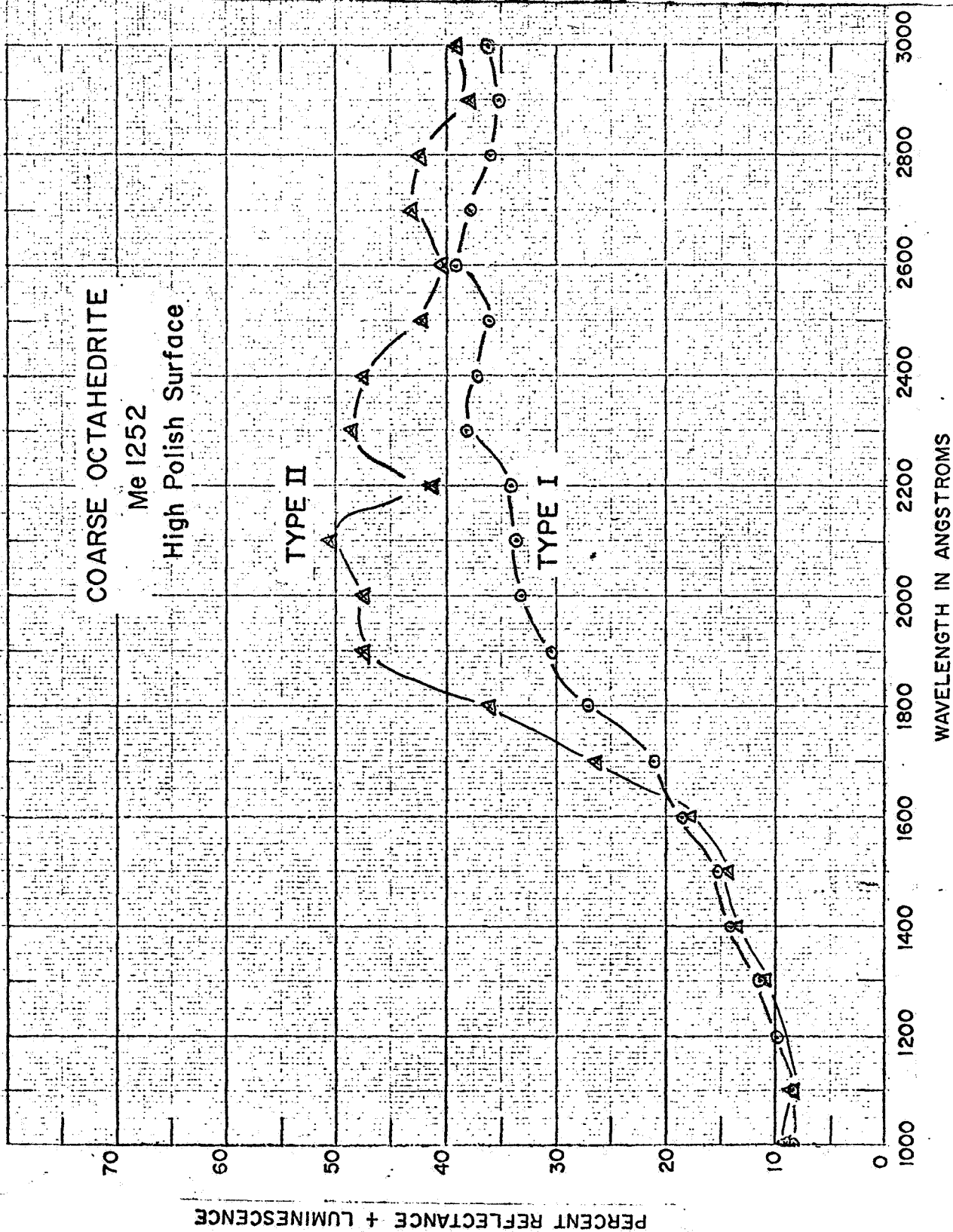


PERCENT REFLECTANCE + LUMINESCENCE

A-18







DISTRIBUTION LIST - TECHNICAL LETTERS

Dr. Richard J. Allenby (2 copies)  
Deputy Director  
Manned Space Science, OSSA  
Code SM, NASA Headquarters  
Washington, D.C. 20546

[REDACTED] (5 copies)  
Program Chief, Earth Resources Survey  
Code SAR, NASA Headquarters  
Washington, D.C. 20546

Mr. A. B. Campbell  
U.S. Geological Survey  
Chief, Northern Rocky Mt. Branch  
Bldg. 25, Federal Center  
Denver, Colorado 80225

Mr. W. D. Carter  
Geology Coordinator  
U.S. Geological Survey  
Rm. B-305, GSA Building  
Washington, D.C. 20242

Mr. Leo F. Childs  
Code TE-2  
NASA Manned Spacecraft Center  
Houston, Texas 77058

Mr. Robert L. Christiansen  
Special Projects Branch  
U. S. Geological Survey  
Bldg. 25, Federal Center  
Denver, Colorado 80225

Dr. Robert Neil Colwell  
Dept. of Forestry  
243 Mulford Hall  
University of California  
Berkeley, California 94720

John E. Cotton  
U.S. Geological Survey  
Water Resources Division  
John F. Kennedy Federal Building  
Boston, Massachusetts 02203

Max Crittenden  
U.S. Geological Survey  
345 Middlefield Road  
Menlo Park, California 94025

John F. Cronin  
Geotechnics Branch  
Terrestrial Science Lab, AFCHL  
Bedford, Mass. 01731

Mr. David F. Davidson  
Chief, Geochemical Census  
U.S. Geological Survey  
Bldg. 25, Federal Center  
Denver, Colorado 80225

Ralph L. Erickson  
U.S. Geological Survey  
Branch of Exploration Research  
Denver, Colorado 80225

Mr. Raymond W. Fary, Jr. (15 copies)  
Chief, RESECS  
U.S. Geological Survey  
801 19th Street, N.W. Room 1032  
Washington, D.C. 20242

Mr. William A. Fischer (2 copies)  
Research Coordinator  
EROS Program/USGS  
Rm. 5226 GSA Building  
Washington, D.C. 20242

Forestry Remote Sensing Lab.  
PSW Forest & Range Exp. Station  
Box 245  
Berkeley, California 94720

Dr. John C. Frye  
State Dept. of Registration & Education  
121 Natural Resources Building  
University of Illinois Campus  
Urbana, Illinois 61801

Dr. Stephen J. Gawarecki  
U.S. Geological Survey  
Rm. 1129 Crystal Plaza  
11th Floor, Building 6  
Arlington, Virginia 22202

Mr. T. George  
Program Manager  
Code SAB/APB & S and Aircraft Program  
NASA Headquarters  
Washington, D.C. 20546

(all persons receive one copy unless otherwise noted)

Dr. Arch Gerlach  
Geography Coordinator  
U.S. Geological Survey  
Rm. 6255, GSA Building  
Washington, D.C. 20242

Arthur Grantz  
U.S. Geological Survey  
345 Middlefield Road  
Menlo Park, California 94025

Gordon Greene  
U.S. Geological Survey  
Crystal Plaza  
11th Floor, Building 6  
Arlington, Virginia 22202

Bernardo Grossling  
U.S. Geological Survey  
RM. 4444 Interior Building  
Washington, D.C. 20240

George Gryc  
U.S. Geological Survey  
345 Middlefield Road  
Menlo Park California 94025

John Hack  
Asst. Chief Geologist  
Regional Geology  
U.S. Geological Survey  
Rm. 4211, GSA Building  
Washington, D.C. 20242

William Hemphill  
U.S. Geological Survey  
Rm. 1123, Crystal Plaza  
11th Floor, Building 6  
Arlington, Virginia 22202

Tom Hendricks  
U.S. Geological Survey  
Federal Center, Building 25  
Denver, Colorado 80225

Mr. Allen V. Heyl  
U.S. Geological Survey  
Building 424  
Agriculture Research Center  
Beltsville, Maryland 20705

Mr. Tom Hughes  
Cartography Coordinator  
U.S. Geological Survey  
1740 Old Chain Bridge Road  
McLean, Virginia 22101

Harold L. James  
Chief Geologist  
U.S. Geological Survey  
Geologic Division  
Rm. 4243, GSA Building  
Washington, D.C. 20242

John E. Johnston  
U.S. Geological Survey/RESECS  
Room 2230, GSA Building  
Washington, D.C. 20242

Montis R. Klepper  
Associate Chief Geologist  
U.S. Geological Survey  
Room 4244, GSA Building  
Washington, D.C. 20242

Mr. Allan Kover  
U.S. Geological Survey  
Regional Geophysics Branch  
Room 413, Blair Building  
Silver Spring, Maryland 20910

Dwight M. Lemmon  
Assistant Chief Geologist  
Engineering Geology/USGS  
Room 4214, GSA Building  
Washington, D.C. 20242

Librarian  
Geological Survey  
Federal Center, Building 25  
Denver, Colorado 80225

Librarian  
U.S. Geological Survey  
Room 1033, GSA Building  
Washington, D.C. 20242

Mr. Ross B. Johnson  
U.S. Geological Survey  
Southern Rocky Mountains  
Building 25, Federal Center  
Denver, Colorado 80225

(all persons receive one copy unless otherwise noted)

Librarian  
U.S. Geological Survey  
Branch of Astrogeology  
601 East Cedar Avenue  
Flagstaff, Arizona 86002

Librarian  
U.S. Geological Survey  
345 Middlefield Road  
Menlo Park, California 94025

Dr. Joseph Lintz, Jr.  
Makay School of Mines  
Reno, Nevada 89507

Paul Lowman  
Goddard Space Flight Center  
Code 640, NASA  
Greenbelt, Maryland 20771

Dr. R.J.P. Lyon (3 copies)  
Chairman Infrared Team  
Geophysics Department  
Stanford University  
Stanford, California 94305

Don R. Mabey  
Chief, Regional Geophysics Branch  
USGS/Federal Center  
Denver, Colorado 80225

Jules A. MacKallor  
U.S. Geological Survey  
801 19th Street, N.W., Room 1032  
Washington, D.C. 20242

Robert McCormick  
Department of the Interior  
Bureau of Mines, Room 2516  
Washington, D.C. 20242

George W. Moore  
U.S. Geological Survey  
c/o Bureau Commercial Fisheries  
Marine Laboratory  
La Jolla, California

Miss Winnie Morgan (2 copies)  
Reports Control Officer  
Grants & Research Contracts, GSSA  
Code 3C, NASA Headquarters  
Washington, D.C. 20546

Mr. Hal T. Morris  
U.S. Geological Survey  
Base Metals Branch  
345 Middlefield Road  
Menlo Park, California 94025

Mr. Robert H. Morris  
U.S. Geological Survey  
Special Projects Branch  
Building 25, Federal Center  
Denver, Colorado 80225

Mr. Robert M. Moxham  
U.S. Geological Survey  
Room 1153, Crystal Plaza  
11th Floor, Building 6  
Arlington, Virginia 22202

Dr. A. B. Park  
Agricultural Research Service O.A.  
U.S. Department of Agriculture  
Washington, D.C. 20250

Dallas Peck Assistant Chief Geologist  
Experimental Geology  
Room 4215, GSA Building  
Washington, D.C. 20242

Dr. William T. Pecora  
Director, USGS  
Room 5243, GSA Building  
Washington, D.C. 20242

Robert W. Poplias  
Chm. Department Geography & Geology  
East Tennessee State University  
Johnson City, Tennessee 37601

Charles Pillmore  
U.S. Geological Survey  
Federal Center  
Denver, Colorado 80225

(all persons receive one copy unless otherwise noted)

J. G. Quade  
Mackay School of Mines  
Reno, Nevada 89507

Robert Reeves  
U.S. Geological Survey  
Room 4201 GSA Building  
Washington, D.C. 20242

Edward Risley  
Earth Sciences, Room 080  
National Academy of Sciences  
2101 Constitution Avenue, N.W.  
Washington, D.C. 20418

Charles J. Robinove  
U.S. Geological Survey  
Water Resources Division  
GSA Building - Room 2226  
Washington, D.C. 20242

Leverett Ropes  
Water Resources Division  
U.S. Geological Survey  
Federal Building  
St. Paul, Minnesota

Mr. Gerald G. Schaber  
U.S. Geological Survey  
Branch of Astrogeology  
601 East Cedar Avenue  
Flagstaff, Arizona 86002

Mr. Daniel R. Shawe  
U.S. Geological Survey  
Light Metals & Industrial Minerals  
Building 25, Federal Center  
Denver, Colorado 80225

Mr. D. B. Simonett  
Geography & Meteorology  
CRES, the University of Kansas  
Lawrence, Kansas 66045

Parke D. Snaveley (2 copies)  
U.S. Geological Survey  
345 Middlefield Road  
Menlo Park, California 94025

Mr. David L. Southwick  
U.S. Geological Survey  
Agriculture Research Center  
Building 420  
Beltsville, Maryland 20705

Ogden L. Tweto  
Assistant Chief Geologist  
Economic Geology/USGS  
Room 4240, GSA Building  
Washington, D.C. 20242

William Vest  
IIT Research Institute  
Suite 300  
1200 17th Street, N.W.  
Washington, D.C. 20036

Mr. R. E. Wallace  
U.S. Geological Survey  
Pacific Coast States Branch  
345 Middlefield Road  
Menlo Park, California 94025

Russell G. Wayland (3 copies)  
USGS/Conservation  
Room 3243, GSA Building  
Washington, D.C. 20242

Prof. E. R. Timothy Whitten  
Geology Department  
Northwestern University  
Evanston, Illinois 60201

Donald R. Wiesnet  
U.S. Geological Survey  
Water Resources Division  
John F. Kennedy Federal Building  
Boston, Massachusetts 02203

Mr. Edward W. Wolfe  
U.S. Geological Survey  
Pacific Coast Branch  
345 Middlefield Road  
Menlo Park, California 94025

Mr. Ed Zeitler  
Code TF2  
Manned Spacecraft Center  
Houston, Texas 77058

Dr. Isidore Zietz  
U.S. Geological Survey  
Regional Geophysics Branch  
Room 415, Blair Building  
Silver Springs, Maryland 20910

H. J. Yatko  
Manager, Spacecraft Oceanography Project  
U.S. Naval Research Lab, Navacano  
Washington, D.C. 20390

(all persons receive one copy unless otherwise noted)